Geopersia 2022, 12(2): 241-264
DOI: 10.22059/GEOPE.2022.339263.648649

RESEARCH PAPER

Structural analysis and the late Cenozoic tectonic evolution of the SE Alborz Mountains in northern Iran: insights into the Arabia-Eurasia collision

Amir Naeimi [1], Seyed Ahmad Alavi [1,*], Saeed Madanipour [2]

[1] Department of Sedimentary Basins and Petroleum, Faculty of Earth Sciences, Shahid Beheshti University, 19839-63113, Tehran, Iran
[2] Department of Geology, Tarbiat Modares University, 14115-175, Tehran, Iran

Received: 19 February 2022, Revised: 02 May 2022, Accepted: 16 May 2022

Abstract
Structural analyses in the SE Alborz Mountains show that the deformation style changes in different parts of the area. In the southwestern parts, presence of a thick succession of low competent middle-upper Eocene to Pliocene layers that include marl and evaporitic rocks have facilitated the occurrence of open to gentle upright folds. However, in the northeast, where a thinner succession of low competent layer is observed, high-angle reverse faults have occurred. The low competent units seem to have deposited in a shallow-water marine basin formed as a result of a regional uplift in response to onset of reverse kinematics on the Bashm Fault during the late Eocene time. The onset of this reverse kinematics is contributed by the collision between the Arabian and Eurasian Plates. As a consequence, our data mainly agrees with the studies proposing the late Eocene-early Oligocene as the time of commencement of the Arabia-Eurasia collision. Additionally, since the SE Alborz Mountains seem to have experienced a prolonged extensional setting during the middle Eocene, the above-mentioned reverse kinematics may indicate a middle Eocene inversion event. Our data also revealed that the late Miocene-late Pliocene was a critical time in the study area, when regional surface uplift took place and substantial clastic materials were shed upon the already folded rock units. A significant episode of deformation may have occurred at this time.

Keywords: SE Alborz Mountains, Deformation Style, High-Angle Reverse Faults, Arabia-Eurasia Collision.

Introduction

Deformation styles may change in the fold and thrust belts normally as a result of pinch-outs of detachment horizons, lateral variations in stratigraphic thicknesses and/or lithologies (Poblet & Lisle, 2011) and sometimes presence of a large-scale structure (Balling et al., 2021). Existence of basement structures and salt can also contribute to deformation style variations and structural complexities in mountain ranges (Yuan et al., 2018). In addition to structural geometry, the amount and rate of the shortening, topography, crustal geometry, denudation (Giambiagi et al., 2012) and foreland sedimentation (Yin, 2006) may also vary in the fold and thrust belts. Deformational changes from folding to dominant thrusting have been witnessed in the Appalachians (Gwinn, 1964), the Canadian Rocky Mountains (Wheeler et al., 1972) and the Cantabrian Mountains (Julivert & Arboleya, 1984) and many other mountain ranges.

In the Alborz Mountains in northern Iran, the Arabia-Eurasia collision and motions of the

* Corresponding author e-mail: a-alavi@sbu.ac.ir

South Caspian Bain toward Iran and Eurasia (see e.g., Jackson et al., 2002; Allen et al., 2003; Vernant et al., 2004a,b; Ritz et al., 2006; Djamour et al., 2010; Khorrami et al., 2019) are generally suggested to explain the tectonic evolution of this range during the late Cenozoic. Here, differences in regional sedimentary basins and general structural trends throughout the belt were proposed by earlier researchers e.g., Stöcklin (1974). Variations in the present-day deformation rates were also discovered through GPS studies (see e.g., Vernant et al., 2004b; Djamour et al., 2010; Khorrami et al., 2019). However, the deformation style variations have scarcely been highlighted particularly in the SE Alborz Mountains. The study area was subdivided by Nabavi (1987) into several subzones whose borders correspond to range-parallel faults e.g. Bashm (BF), Anzab (AnF), Abbassabad (AbF), Peyghambaran (PF), Diktash (DF), and North Semnan (NSF) (Figs. 2 and 3). However, such a division has been poorly supported by structural analyses. In this paper we want to decipher what contributed to the differences in the deformation style of the SE Alborz Mountains. The late Cenozoic structural evolution of the region and the role major faults played in this respect are also investigated based on combined field observations and available data. We also shed light on the timing of the collision between the Arabian and Eurasian Plates which has been a matter of the debate over the past years (see e.g., Koshnaw et al., 2018 and the references therein).

Tectonic and geological setting

As a double-verging arcuate mountain belt in northern Iran (Fig. 1), the Alborz Mountains are located between the Kopeh Dagh and Talesh mountain ranges to the northwest and northeast, respectively, and two foreland basins i.e. the South Caspian Basin and the Central Basin of Iranian Plateau in the north and in the south, respectively (Jackson et al., 2002; Allen et al., 2003; Madanipour et al., 2017; Mattei et al., 2017, 2019; Naeimi et al., 2022). Formation and then inversion of several subbasins (e.g., Zanchi et al., 2006; Ballato et al., 2011), fault kinematic reversals (Yassaghi & Madanipour, 2008; Yassaghi & Naeimi, 2011; Ehteshami-Moinabadi, 2014; Javadi et al., 2020) and rapid cooling events (e.g., Axen et al., 2001; Guest et al., 2006b; Rezaeian et al., 2012; Shafiei Bafti et al., 2021) are clear evidence for multiple tectonic events that have affected the range over the ages (Alavi, 1996; Guest et al., 2006a; Shahidi, 2008; Zanchi et al., 2009; Ballato et al., 2011) (Fig. 4a). The Alborz range has been subject to shortening since the late Cenozoic (Guest et al., 2006a,b; Ballato et al., 2011), but the present-day deformation style is represented by the range-parallel thrusting and left-lateral strike-slip faulting (Jackson et al., 2002; Allen et al., 2003; Berberian & Walker, 2010).

In northern Iran, the Eo-Cimmerian orogeny during the Late Triassic represents collision of the Cimmerian blocks (including Iran) with Eurasian Plate and resultant closure of the Paleo-Tethys Ocean (Muttoni et al., 2009a,b; Zanchi et al., 2009) that had opened during the Late Ordovician and Silurian in northern Gondwana between these two (Stampfli & Borel, 2002). Opening of the Neo-Tethys Ocean in the southwestern Iran was another result of this event (see e.g., Zanchi et al., 2009). The syn-to post orogenic Upper Triassic-Middle Jurassic siliciclastic Shemshak Group unconformably overlies the siliciclastic, dolomitic and carbonate rocks of Neoprotrozoic to Lower Triassic age including the Kahar, Soltanieh, Barut, Zagun, Lalun, Mila, Jeirud, Mobarak, Dorud, Ruteh, Nessen and Elika formtions (Fig. 4a) (Stöcklin et al., 1964; Alavi, 1996; Fürsich et al., 2009a; Zanchi et al., 2009; Wilmsen et al., 2009).

During the Middle-Late Jurassic, northern Iran went through regional rifting and then sea-floor spreading processes which led to development of the oceanic South Caspian Basin (Wilmsen et al., 2009; Fürsich et al., 2009b). From the Middle Jurassic to Late Cretaceous, the carbonate-dominated Dalichai, Lar, Tizkuh formations as well as several other unnamed rock units were deposited in the Alborz Mountains (Alavi, 1996; Aghanabati, 2004). They were intensely deformed before the Paleocene terrestrial Fajan Formation and lower Eocene carbonate Ziarat began to accumulate (Guest et al., 2006a; Ballato et al., 2011). These two formations are overlain by mostly volcaniclastic rocks of the middle Eocene Karaj Formation characterizing an extensional back-arc basin in the north of the Arabia-Eurasia subduction zone (e.g., Brunet et al., 2003; Vincent et al., 2005; Verdel, 2008; Shahidi, 2008; Ballato et al., 2011). During the late Eocene to early Oligocene a shallow-water marine setting (Assereto, 1966) began to exist in the southern Central Alborz where sandstone, siltstone, shale, gypsum, marly limestone and marl were deposited (Nabavi, 1987; Aghanabati & Hamedi, 1994; Ballato et al., 2008).

In the Central and southern Alborz Mountains, the Oligocene clastic rocks equivalent to the Lower Red Formation (LRF) of the Central Basin (e.g., Ballato et al., 2011) unconformably overlie the middle to upper Eocene units. Here, the LRF underlies the Oligo-Miocene marine Qom Formation (QF) (e.g., Bozorgnia, 1966; Reuter et al., 2007) that in turn is covered by a red clastic unit known as the Upper Red Formation (URF) (Amini, 1997). The URF has evidence for foreland basins development along the southern flank of the Alborz Mountains (Ballato et al., 2008). Intermontane basins are suggested to have been filled at this time in the Western Alborz (Guest et al., 2007) and Tarom Basin (Paknia et al., 2021). The synorogenic clastic deposits of the Hezardarreh and Kahrizak formations as well as recent sediments cover the URF and older rock units in the southern Central Alborz (e.g., Rieben, 1955; Ballato et al., 2008). These Pliocene to Quaternary deposits are currently actively being deformed and uplifted by seimogenic faults (e.g., Tchalenko et al., 1974; Solaymani Azad et al., 2011; Talebian et al., 2016).

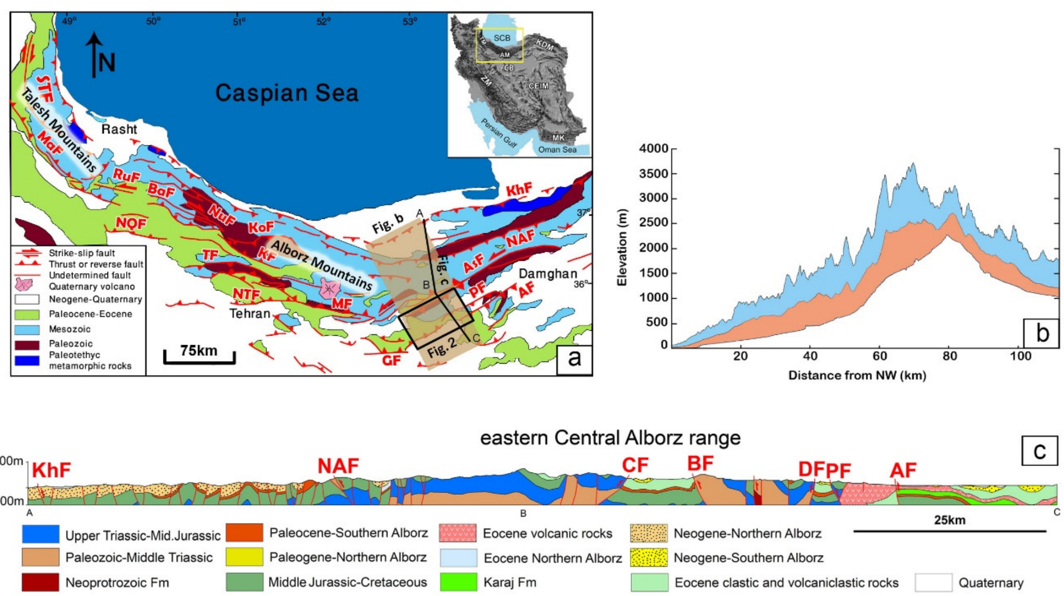

Figure 1. Simplified tectonic map of the Alborz and Talesh Mountains modified from Zanchi et al., (2006). The box refers to the study area. Abbreviations: AF: Attary Fault; AsF: Astaneh Fault; BaF: Banan Fault; BF: Bashm Fault; CF: Chashm Fault; DF: Diktash Fault; GF: Garmsar Fault; KF: Kandovan Fault; KhF: Khazar Fault; KoF: Kojour Fault; MaF: Masuleh Fault; MF: Mosha Fault; NAF: North Alborz Fault; NQF: North Qazvin Fault; NTF: North Tehran Fault; NuF: Nusha Fault; PF: Peyghambaran Fault; RuF: Rudbar; STF: South Talesh Fault; TF: Taleghan Fault. Inset: major tectonic zones of Iran. Yellow rectangle shows Alborz-Talesh Mountains. AM: Alborz Mountains; CB: Central Basin; CEIM: Central-Eastern Iranian Microcontinent; MK: Makran accretionary prism; KDM: Kopeh Dagh Mountains; TM: Talesh Mountains; SCB: South Caspian Basin; ZM: Zagros Mountains. (b) A Swath profile showing minimum, maximum and mean elevation along the eastern Central Alborz range. (c) A regional cross section across the eastern Central Alborz. The Geology is modified after Vahdati Daneshmand & Saidi (1991) and Aghanabati & Hamedi (1994)

Stratigraphy of the SE Alborz Mountains

In the study area, the Lower Cambrian to Quaternary deposits have outcrops (Figs. 2, 4b and 5), but the oldest rock units are the thick-bedded black dolomites of the Soltanieh Formation ($Є_s$) in the hanging wall of the AnF (Fig. 5a). In the hanging wall of the BF, the Barut Formation is at least ~1400m thick. It conformably underlies the > ~700m-thick siliciclastic Zagun - Lalun Formations. In most places, the Mila Formation ($Є_m$) composed of dolomite, limestone, shale and sandstone (Fig. 5b) overlies the Lalun Formation with a white quartz arenite unit known as "top quartzite" at the base (see e.g., Stöcklin et al., 1964). Geyer et al., (2014) recommended that the Mila Formation might be subdivided into several formations and compose a group.

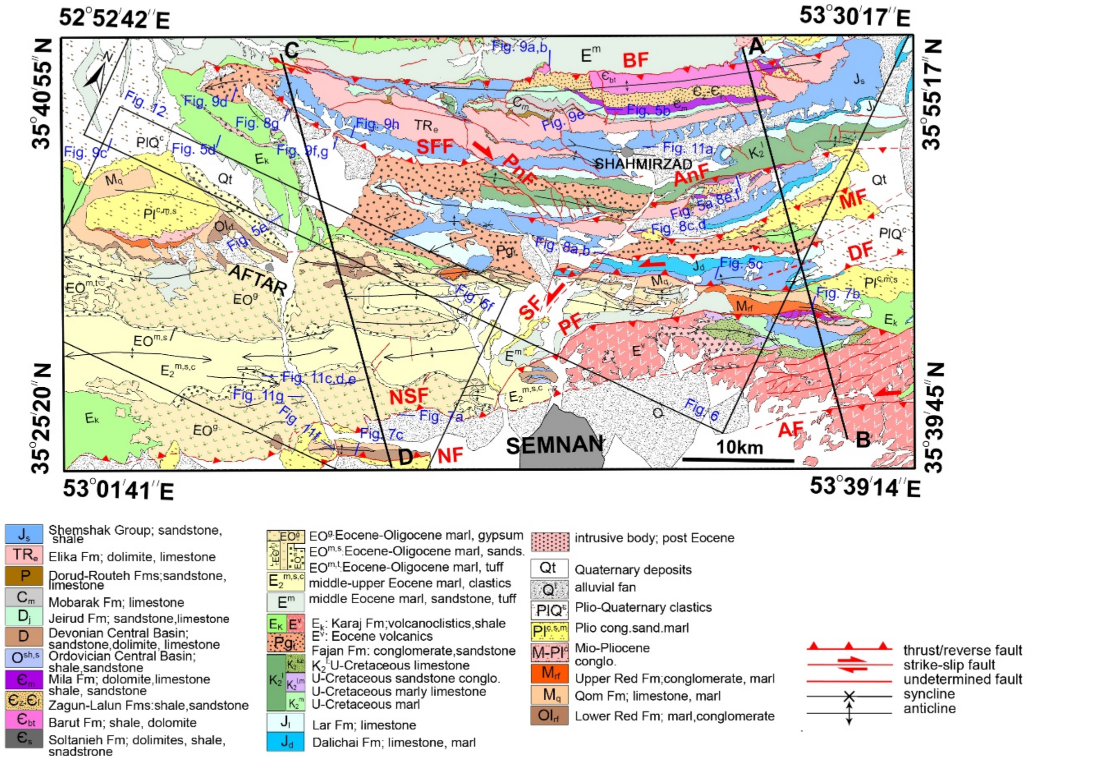

Figure 2. A simplified geological map of the study area modified after Nabavi (1987) and Aghanbati & Hamedi (1994). The locations of the figures are indicated in blue. Abbreviations: AF: Attary Fault; AbF: Abbassabad Fault; AnF: Anzab Fault; BF: Bashm Fault; DF: Diktash Fault; MF: Mahdishahr Fault; NF: Namakdan Fault; NSF: North Semnan Fault; PF: Peyghambaran Fault; PnF: Peno Fault; SF: Sangsar Fault; SFF: Sefidab Fault

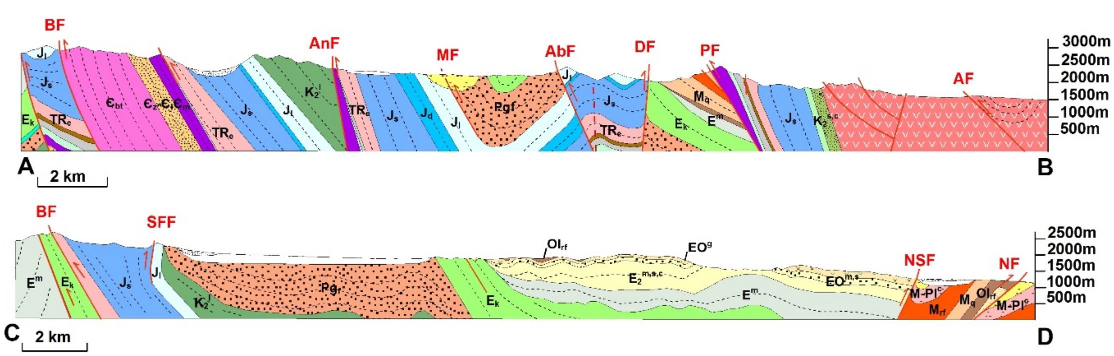

Figure 3. Cross section across the paths outlined in 3. The Cross section A-B is partly modified after Naeimi et al., (2022). The legend is the same as the one in Fig. 2

Accordingly, they suggested the Fasham Formation includes the top quartzite unit. The middle to upper Paleozoic units underlie the Elika Formation which in turn is covered by the Shemshak Group. In the southeast, the lower Paleozoic succession appears again within the hanging wall of the PF. Here, the Mila Formation is oldest unit overlain by the Jeirud Formation.

The Shemshak Group consisting of sandstone, shale and siltstone (Fig. 5c) underlies the marly limestones of the Dalichi Formation that is mostly thinned and merged with lowest parts of the carbonate Lar Formation. In the study area, the Lower Cretaceous Tizkuh Formation has been intensively eroded and its outcrops are mainly absent (Nabavi, 1987; Alavi-Naini, 1972, 1997). The Upper Cretaceous rock units are observed only in the hanging wall of the BF and PF. However, their contents are not the same. In the former, the rock units are mostly carbonate, but in the latter sandstone and marl are dominant. Resting over the folded and faulted Cretaceous and even older formations, the >1000m-thick Fajan Formation contains red terrestrial conglomerate and sandstone. In the hanging wall of the PF, this formation seems to have been intensively eroded. In the study area, the lower Eocene Ziarat Formation is very rare and not commonly observed except for footwall of the PF. In the southwest of the study area, the Fajan Formation is mostly overlain by tuff and shale of the Karaj Formation (E_k) (Fig. 5d). A thick pile of Eocene volcanic rocks is observed in the southeast of the area (Alavi-Naini, 1997) (Fig. 2).

According to Ballato et al., (2011) a transition from volcaniclastic submarine deposits to shallow-water marine evaporitic and terrestrial sediments occurred shortly after 36 Ma. As a result, a ~2500-3000 m-thick succession of middle-upper Eocene marl and clastic rocks cover the Karaj Formation that is most cropping out in west of the study area. Here, a local angular unconformity exists between the middle Eocene marl, sandstone and tuff (E^m) and the upper Eocene-Oligocene marl and sandstone ($EO^{m,s}$) (Fig. 5e). Nabavi (1987) also reported a local angular unconformity between the middle-upper Eocene marl and clastic rocks ($E_2^{m,s,c}$) and older rock units at the south-central parts of the study area (Fig. 2).

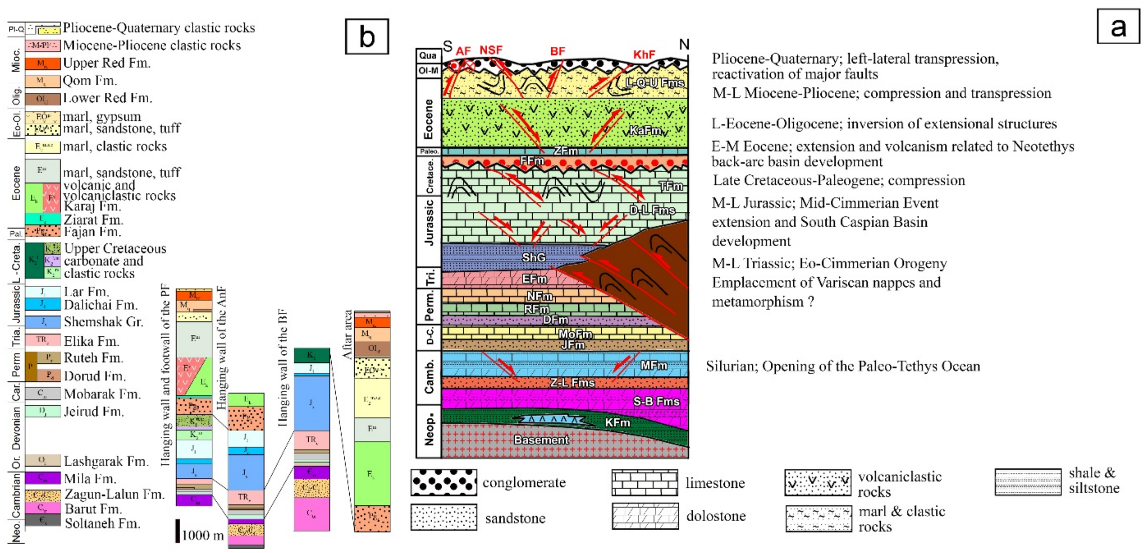

Figure 4. (a) Tectonostratigraphic column of the Central Alborz (modified after Allen et al., 2003; Guest et al., 2006a; Madanipour et al., 2017). See the text for discussion. Abbreviations: KFm: Kahar Formation; S-B Fms: Soltanieh and Barut Formations; Z-L Fms: Zagun and Lalun Formations; MFm: Mila Formation; JFm: Jeirud Formation; MoFm: Mobarak Formation; DFm: Dorud Formation; RFm: Ruteh Formation; NFm: Nessen Formation; EFm: Elika Formation; ShG: Shemshak Group; D-L Fms: Dalichai and Lar Formations; TFm: Tizkuh Formation; FFm: Fajan Formation; ZFm: Ziarat Formation; KaFm: Karaj Formation; L-Q-U Fm: Lower Red, Qom and Upper Red Formatiom. The rest of the column is unnamed rock units. (b) Simplified stratigraphic columns in different parts of the study area (modified after Nabavi (1987) and Alavi-Naini (1997))

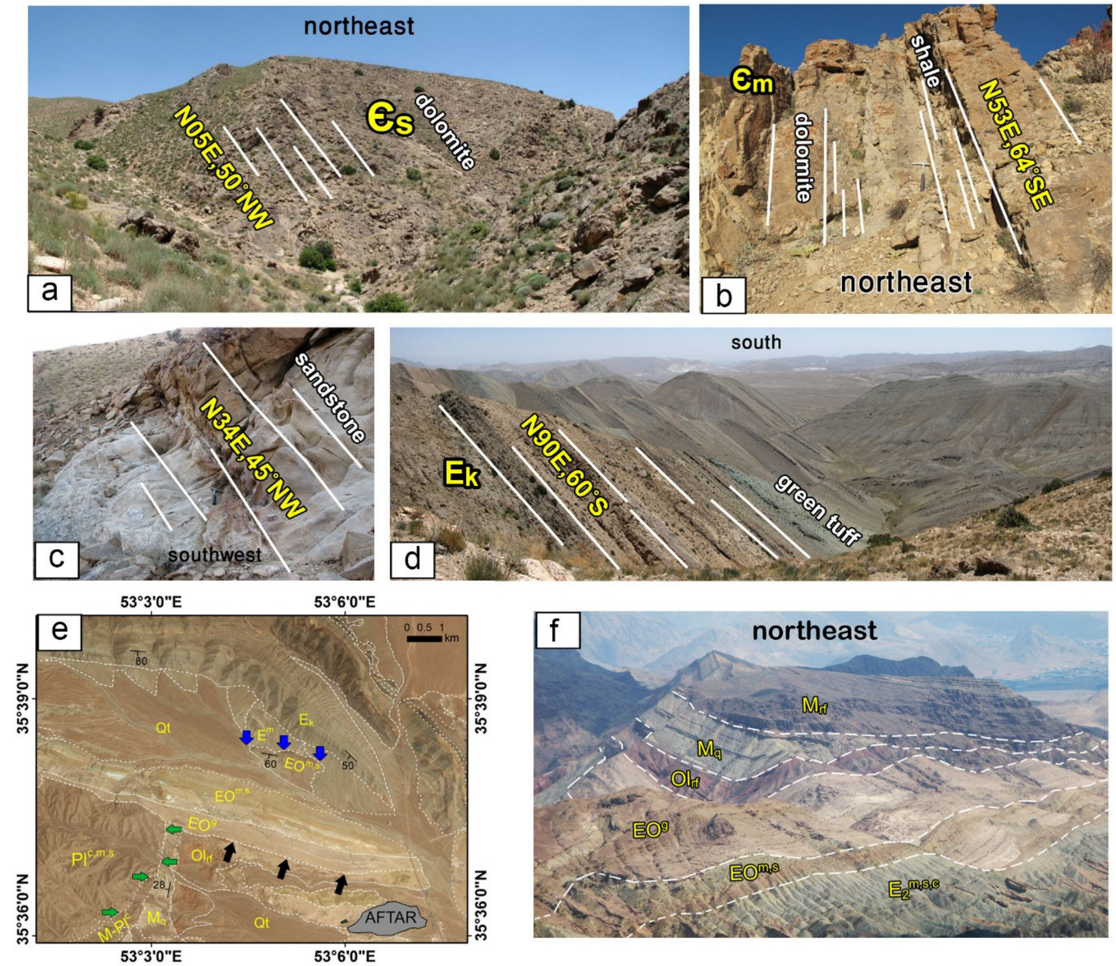

Figure 5. (a) The black thick-bedded dolomites of the Soltanieh Formation ($Є_s$) in the hanging wall of the AnF. The dip of the bedding planes is indicated in yellow. (b) The Mila Formation ($Є_m$) in the hanging wall of the BF comprises dolomite, limestone, sandstone and shale. The dip and traces of the bedding planes are indicated. (c) Thick-bedded sandstones alternate with shale and siltstone in the Shemshak Group in the hanging wall of the DF. The dip and traces of the bedding planes are indicated. (d) The green tuff and shale are main lithologies of the Karaj Formation (E_k) in the study area. The dip and traces of the bedding planes are indicated. (e) The local angular unconformity (marked by blue arrows) between the upper Eocene-Oligocene marl and clastic rocks ($EO^{m,s}$) and middle Eocene marls (E^m). The LRF and QF (Ol_{rf} and M_q) are also observed resting on the upper Eocene-Oligocene marl and gypsum (EO^g) with another angular unconformity (marked by black arrows). A third angular unconformity (green arrows) is witnessed between Pliocene clastic rocks ($Pl^{c,m,s}$) and older formations. (f) Further east, there is no sharp angular unconformity between these formations

The middle to upper (?) marl and clastic rocks are followed by an 80-100m thick unit composed of upper Eocene-Oligocene marl and large volumes of gypsum (EO^g). To the northeast, this sequence is thinned and the Karaj Formation is covered by the QF (cross section A-B in Fig. 3). Collectively, it seems that by the late Eocene, the submarine eruptions had already vanished and the southeastern third of the SE Alborz had turned into a shallow-water marine basin suitable for evaporitic deposition.

The LRF (~600m thick), QF(~600m thick) and URF (~400m thick) have outcrops in the southeastern third of the study area. Here, the QF is early Miocene in age (Nabavi 1987; Alavi-Naini, 1997). In the southwest, the LRF and QF (Ol_{rf} and M_q) are seen occasionally resting upon the older rock units for instance EO^g (Fig. 5e) with an angular unconformity. However, there is no sharp angular unconformity between these formations further east (Fig. 5f). The URF was deposited from17.5 to 7.5 Ma (Ballato et al., 2008) showing that the foreland basins had already began to form to the south of the Alborz Mountains (Amini, 1997; Ballato et al., 2008). Pliocene marl and conglomerates and Plio-Quaternary to recent deposits overlie the older deposits with an angular unconformity (Fig. 5e).

Structures

In the study area the major faults run NE-SW and exhibit reverse kinematics that is sometimes accompanied by strike-slip components of slip (Figs. 2, 3 and 6). In the Alborz range, the range-parallel thrust faults are considered the prominent structures (Allen et al., 2003; Yassaghi, 2005; Yassaghi & Naeimi, 2011) and sources of earthquakes (SoltaniMoghadam et al., 2019). Together with associated active anticlines and synclines they accommodate almost all shortening across the belt (Yassaghi, 2005; Ghassemi, 2005; Nazari, 2006). They may exhibit evolution history of the belt by kinematic and geometric changes (Yassaghi & Madanipor, 2008; Yassaghi & Naeimi, 2011; Javadi et al., 2020). Folding is also widespread in this area. The data concerned with geometry of the structures and the measurement stations are provided in Table 1.

Table 1. Structural data and location of measurement stations

Station No	Latitude	Longitude	Measured Structure	Averaged attitude	(Averaged) Fault/Shear Plane	Aixal Plane	Fold Axis
1	35° 43' 2.5411" N	53° 01' 43.9012" E	Bashm Fault		N84E,66˚SE		
2	35° 44' 17.6519" N	53° 06' 11.2194" E	Bashm Fault		N25E,75˚SE		
3	35° 44' 37.9888" N	53° 07' 27.5060" E	Bashm Fault		N38E,75˚SE		
4	35° 48' 3.6462" N	53° 14' 52.7901" E	Bashm Fault		N58E,58˚SE		
5	35° 49' 38.5013" N	53° 19' 52.3226" E	Bashm Fault		N44E,66˚SE		
6	35° 48' 1.7272" N	53° 17' 10.0803" E	A transversal fault		N20W,65˚SW		
7	35° 47' 47.8493" N	53° 17' 50.2942" E	A transversal fault		N48W,86˚NE		
8	35° 45' 19.6821" N	53° 18' 20.7576" E	Kuh-e-Lahard Anticline			N73E, 88˚SE	03˚, N83E
9	35° 45' 50.3424" N	53° 18' 31.2379" E	Kuh-e-Lahard Syncline			N73E, 72˚ NW	11˚, N69E
10	35° 47' 11.6773" N	53° 25' 2.1735" E	Anzab Fault		N71E, 85˚SE		
11	35° 37' 37.9234" N	53° 10' 30.6146" E	Kuh-e-Gachi Syncline			N58E, 90˚NW	09˚, S58˚W
12	35° 43' 26.6229" N	53° 21' 43.7971" E	Mahdishahr Fault		N81E,72˚SE		
13	35° 45' 45.3626" N	53° 28' 14.5632" E	Abbassabad Syncline			N40E, 84˚NW	11˚, N39E
14	35° 42' 18.6001" N	53° 21' 24.3232" E	Abbassabad Fault		N79E,66˚SE		
15	35° 42' 57.1370" N	53° 26' 32.4373" E	Diktash fault		N51E,89˚NW		
16	35° 42' 55.0127" N	53° 29' 49.1286" E	Peyghambaran Fault		N51E, 72°SE		
17	35° 36' 39.1994" N	53° 11' 15.0611" E	Cheshmeh Shirin Anticline			N72E, 90˚NW	05˚, S72W
18	35° 34' 45.5755" N	53° 10' 26.0825" E	Kuh-e-Sefid Syncline			N51E, 89˚NW	01˚, S51W
19	35° 34' 56.8758" N	53° 13' 47.6622" E	Eskadar Anticline			N61E, 82˚NW	00˚, S61W
20	35° 33' 26.8676" N	53° 09' 38.5202" E	Golroo Anticline			N50E, 83˚NW	06˚, N49E
21	35° 32' 1.4160" N	53° 08' 57.7823" E	Siyahsuk Anticline			N68E,79˚N W	15˚, N65E
22	35° 30' 49.7136" N	53° 13' 17.2836" E	Namakdan Anticline			N64E, 86˚NW	05˚, S64W
23	35° 42' 0.0625" N	53° 06' 46.0350" E	A transversal fault		N12E,61˚SE		
24	35° 50' 39.9659" N	53° 25' 42.5283" E	Pingareh Fault		N48E,70˚SE		
25	35° 51' 25.6954" N	53° 24' 47.3618" E	Perous Fault		N83E,78˚SE		
26	35° 51' 36.9045" N	53° 23' 45.0785" E	Bashm Fault		N84E,82˚SE		
27	35° 41' 28.8118" N	53° 02' 55.8423" E	Akhorchal Syncline			N83W,75˚ NW	27˚, S75E
28	35° 46' 5.3357" N	35° 46' 5.3357" N	Bashm Fault	N32E, 62°SE			
29	35° 42' 19.5861" N	53° 01' 31.6318" E	Post-Eocene dikes	N-05W			
30	35° 42' 10.0387" N	53° 04' 15.9468" E	Sefidab Fault		N77E, 30°NW		
31	35° 43' 21.1103" N	53° 26' 43.9532" E	Diktash Anticline			N53E,80˚N W	25˚, S58W

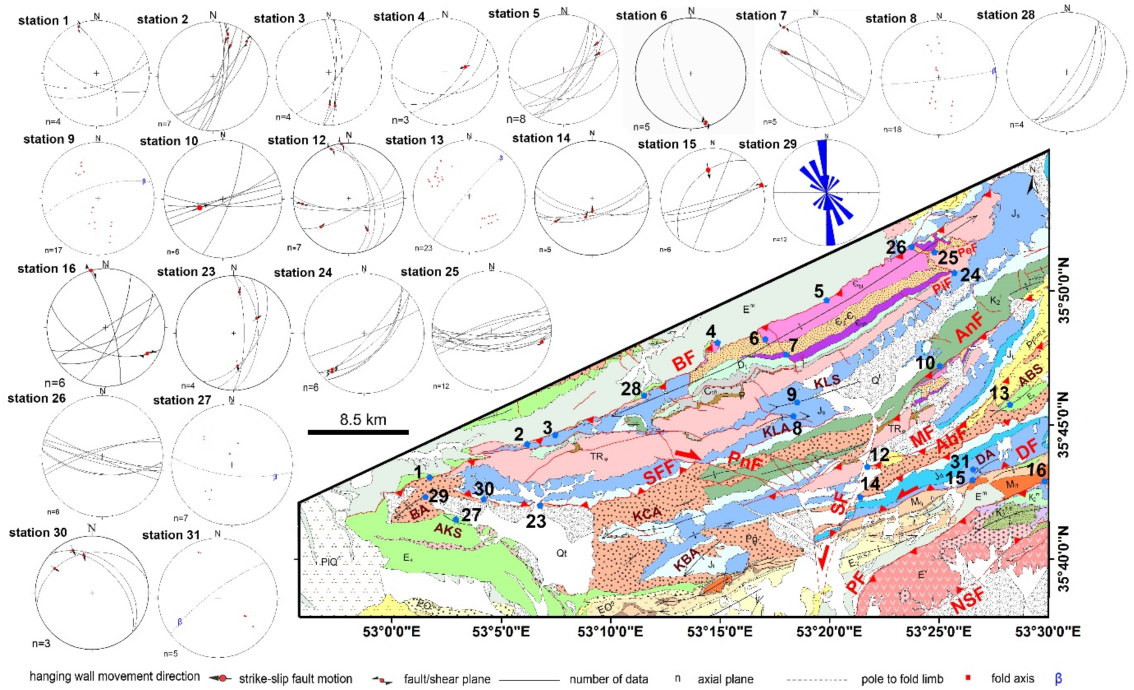

Figure 6. A simplified geological map showing the structures devolved in central-eastern parts of the study area. The measurement stations are indicated as blue pentagonals and black bold numbers. Stereonet plots are provided for each station. Abbreviations: AF: Attary Fault; AbF: Abbassabad Fault; ABS: Abbassabad Syncline; AnF: Anzab Fault; AKS: Akhorchal Syncline; BA: Bashm Anticline; BF: Bashm Fault; DF; Diktash Anticline; DF; Diktash Fault; KBA: Kelyab Anticline; KCA: Kuh-e-Chenaran Anticline; KLA: Kuh-e-Lahard Anticline; KLS: Kuh-e-Lahard Synicline; MF: Mahdishahr Fault; NSF: North Semnan Fault; PF: Peyghambaran Fault; PeF: Perous Fault; PiF: Pingareh Fault; PnF: Peno Fault; SF: Sangsar Fault; SFF: Sefidab Fault. The legend is the same as the one in Fig. 2

Major faults

Bordering the southern limits of the SE Alborz Mountains, the range-front NSF places Cenozoic units over the Quaternary deposits (Nabavi 1987; Berberian et al., 1996) (Fig. 7a). The NSF dips steeply to the northwest and is suggested to be deep-seated with evidence of microseimicity (Nemati et al., 2011). Naeimi et al., (2022) suggested that NSF is most responsible for outward growth and thrust loading in the SE Alborz Mountains. In the hanging wall of the NSF, there is the PF (station 16 in Fig. 6) that is a ~36 km-long back thrust placing the lower Paleozoic to Eocene formations over several younger rock units (e.g., the QF and URF) (Fig. 7b). In the east, the fault finally vanishes in the Karaj Formation, but in the west, the PF is linked to the NSF and giving rise to out crops of the Central Basin formations e. g. Devonian rocks within the hanging wall (Fig. 2). The NSF is also linked to the Namakdan Fault (NF) that is one of latest faults that formed in this region (Fig. 7c). The marl, sandstone and evaporitic rocks of the LRF are folded (Namakdan Anticline; NA) and thrust upon the Quaternary deposits by this NW-dipping thrust fault.

To the north of the PF, lies the DF (Fig. 6) that is a ~27 km long, NW-dipping fault thrusting the Mesozoic formations over Paleocene, Eocene, Oligocene and Miocene units. In the hanging wall, only the Upper Triassic to Upper Jurassic units (i. e. the Shemshak Group, the Dalichai and Lar Formations) crop out, indicating a moderate vertical displacement of the DF or less structurally-controlled exhumation. The straight fault trace (Figs. 2 and 6) plus high-angle shear planes (Fig. 7d) represent the high angle dip of the fault (station 15 in Fig. 6). There are even SE-dipping shear planes in the fault zone. A moderate to large left-lateral component of slip accompanies the reverse kinematics. Further northeast, a rather large alluvial fan is uplifted by a fault and cut by another fault, suggesting that deformation is still going on in this part of the Alborz range (Fig. 7e).

Toward the north, the Fajan Formation is thrust by the Lar Formation along the AbF (Figs. 8a and b). It is a ~34 km-long reverse fault that steeply dips to the southeast (station 14 in Fig. 6). The slickenlines measured on the shear planes indicate that a small component of left-lateral motion accompanies the reverse kinematics. The Fajan Formation also seems to have been partly driven on the older Lar Formation via the ~ 18.5 km-long high-angle Mahdishar Fault (MF) (Fig. 8c; station 12 in Fig. 6) on which some striations show a large right-lateral component of slip (Fig. 8d). In the northeast of the study area, the ~22.5 km-long AnF is also a SE-dipping high-angle reverse fault. In the east, the fault thrusts the earliest Cambrian Soltanieh Formation over the Upper Cretaceous limestones (Fig. 8e), with a moderate left-lateral component of slip, although shear sense indicators are rarely witnessed in the fault zone (Fig. 8f) (station 10 in Fig. 6). However, the AnF places the Elika Formation on the Shemshak Group in the west. The fault and the units in the hanging wall are displaced left-laterally by the transversal Sangsar Fault.

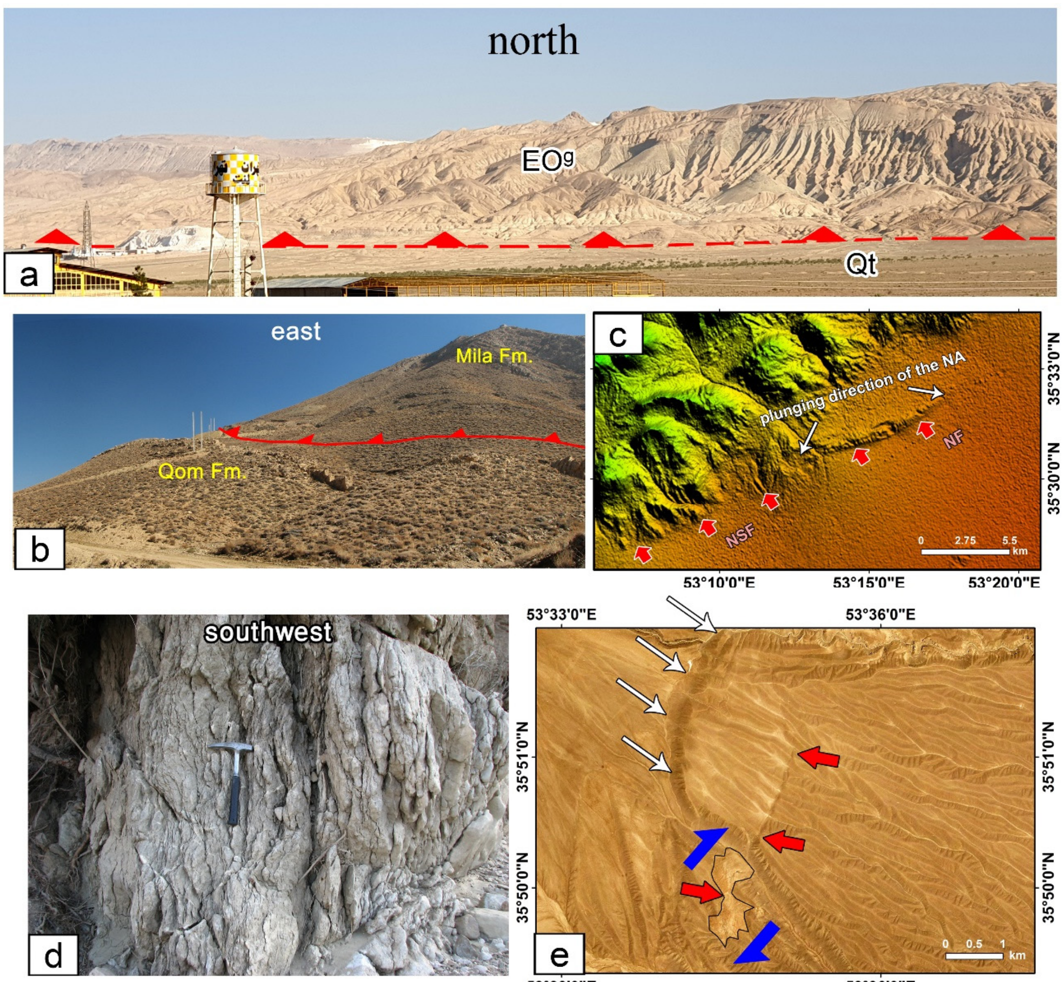

Figure 7. (a) The NSF is a reverse fault placing Eocene to Oligocene units over the Pliocene and even Quaternary deposits. (b) The Mila Formation is thrust upon QF by the PF. (c) Dem 30m of the southeast of the SE Alborz shows active thrusting (red arrows) and folding (white arrows) along the south margin of the SE Alborz, indicating that the range growth is going on. (d) High-angle shear planes developed in the QF within fault zone of the DF. (e) A large alluvial fan is uplifted by a fault (marked by white arrows) and cut by another fault (marked by red arrows), postdating other known structures in the SE Alborz Mountains

To the northwest, Berberian et al., (1996) introduced the Sefidab Fault (SFF) that is a ~22.5km-long reverse fault measured to be N60W, 38°NE (SFF) (Fig. 8g; station 30 in Fig. 6). However, as it is outlined in the cross section C-D, the SFF does not seem to be deep-seated, and has possibly formed due to of rotations in western block of the transversal Peno Fault (PnF) and inevitable motions of the Lar Formation upon the Fajan Formation.

As the prominent structure of the SE Alborz Mountains, the BF is a high-angle reverse fault dipping at ~58-82˚ to the southeast (stations 1,2,3,4, 5, 26 and 28 in Fig. 6). Formations with ages ranging from Lower Cambrian to Paleocene (Figs. 9a and b) have been thrust over the middle Eocene units. Pure strike-slip shear planes are also observed in the fault zones. The units within the hanging wall form a giant anticline whose northern limb is completely cut by the BF. The giant anticline noses can be represented by folding of the Shemshak Group and Fajan Formation in eastern and western tips of the BF, respectively (Figs. 2 and 6).

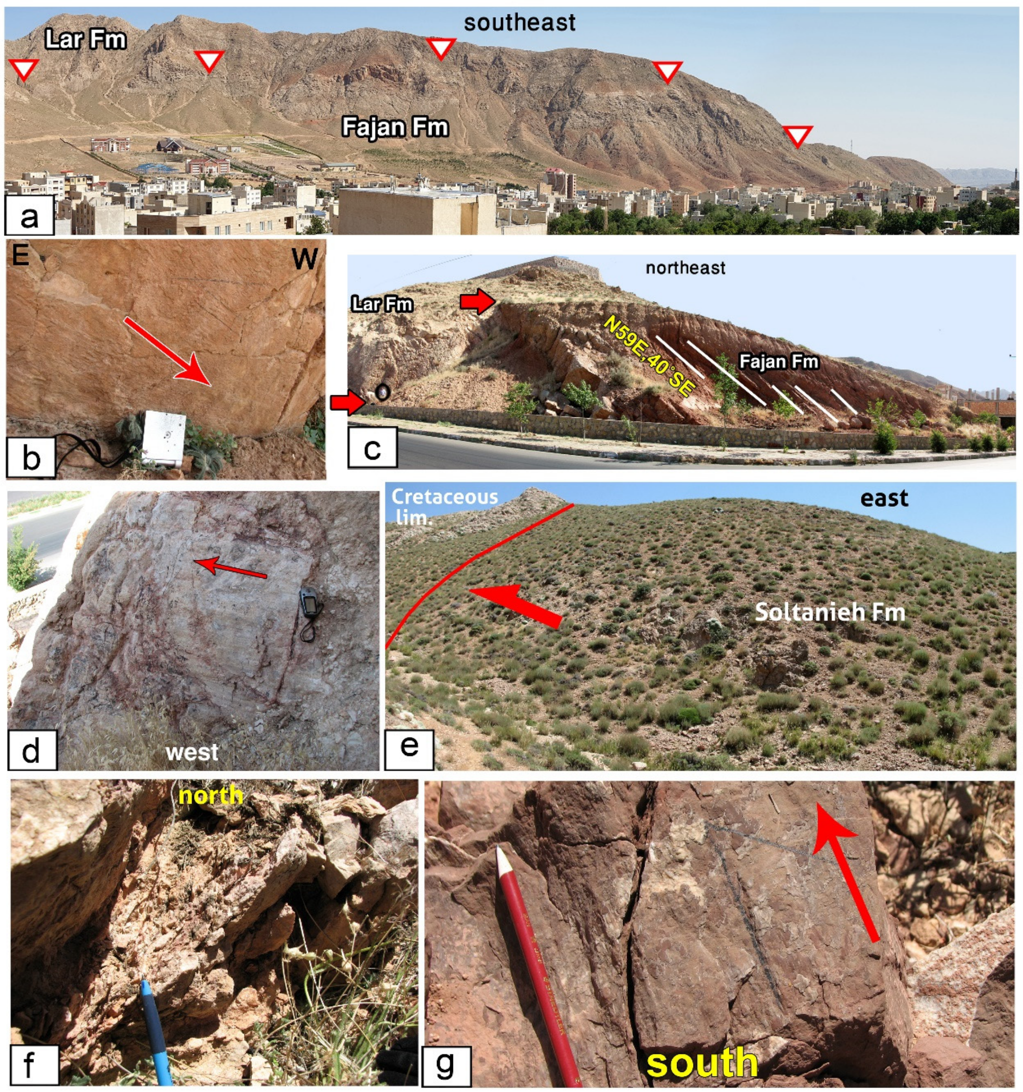

Figure 8. (a) The AbF thrusts the Lar Formation over the Fajan Formation. The white triangles mark the fault trace. (b) A shear plane within the AbF fault zone. The movement of the missing block is shown by a red arrow. (c) The MF has thrust the Fajan Formation upon the Lar Formation. (d) The right-lateral slickenlines on a fault plane within the MF fault zone. The movement of the missing block is shown by a red arrow. (e) The AnF has placed the Soltanieh Formation over the Cretaceous limestones. (f) The shear planes observed in the AnF fault zone. (g) A shear plane measured in the fault zone of the Sefidab Fault

There is no Oligocene unit in the footwall of the BF and it may be concluded the fault has changed the sedimentational environment of the footwall area by the late Eocene time. To the northeast, the BF is linked to the Sabur Fault that thrusts Paleozoic formations upon the Pliocene deposits in southern slopes of the Astaneh valley (Vahdati Daneshmand, 1990). To the southwest, the BF is covered by the Quaternary deposits and in is not clear whether the fault joins other structures or it simply dies out. According to the aeromagnetic map of Semnan quadrangle, the BF is partly corresponding to a magnetic anomaly located in the basement (Yousefi & Friedberg, 1977), leading one to interpret that the BF might be a deep-seated structure in the north of the study area. The BF is also a segment of the left-lateral Shahrud Fault System that is a range-parallel regional feature responsible for accommodating strike-slip component of present-day deformation in the Eastern Alborz (Hollingsworth et al., 2006, 2010; Nemati et al., 2011). However, not many major microseismic events (Nemati et al., 2011; SoltaniMoghadam et al., 2019) nor Quaternary strike-slip evidence are observed along the fault. Instead, deeply incised Plio-Quaternary deposits in the western tip of the fault (Fig. 9c) indicates that the BF is accommodating shortening and surface uplift rather that strike-slip deformation. There are several subsidiary faults associated with the BF. For example, the Pingareh Fault (station 24 in Fig. 6) runs between the Elika and Mila formations. The Perous Fault (station 25 in Fig. 6) is a right-lateral fault juxtaposing the Elika Formation to the Lalun Formation. In hanging wall area of the BF, a number of dikes have intruded into the Paleocene Fajan Formation and the middle Eocene Karaj Formation (Fig. 9d). They are diabasic in content (station 29 in the Fig. 6) and have an averaged trend of N05W compatible with a post-Eocene NNW-oriented compression.

The strike-slip faults cross cutting other structures are NE or NW-trending with left-lateral or right-lateral kinematics, respectively (Fig. 9e). They mostly postdate the major known faults and may also support a post-Eocene NNW-oriented compression. For instance, in the hanging wall of the BF, a right-lateral fault has offset the Paleozoic formations by ~500 m (station 7 in the Fig. 6). The fault depicted in Fig (9f) has an attitude of N12˚E, 61˚SE (station 23 in Fig. 6) and a well-developed fault zone in which share planes are witnessed (Fig. 9g). It left-laterally cuts the Fajan Formation. Numerous minor faults are witnessed all over the area (Fig. 9h). However, the most prominent transversal fault is the ~13 km-long Sangsar Fault (SF) (Fig. 10a) that has left-laterally displaced the AnF, AbF and DF by ~2-3 km at the center of the study area. The Peno Fault (PnF) is another transversal fault that trends WNW-ESE and responsible for ~2km right-lateral offset and rotation of the base of the Fajan Formation (Fig. 10b).

Folding

Folding is particularly observed in the SE Alborz Mountains (Figs. 6, 11 and 12). In northern parts, the Shemshak Group and Karaj Formations are the most folded deposits. For example, the Akhorchal (station 27 in Fig. 6) has deformed the Karaj Formation as a subvertical open syncline whose axis gently plunges to ESE. Toward the east, the city of Shahmirzad has been built upon the folded Shemshak Group. The two most significant folds are the NE-SW-trending Kuh-e-Lahard Anticline (station 8 in Fig. 6) and Kuh-e-Lahard Syncline (station 9 in Fig. 6) whose axes gently plunge to the east. Here, a pair of anticline and syncline is also seen in the Shemshak Group (Fig. 11a). Their folds' axial traces are NE-SW-trending with axes gently plunging to the northeast. In the east of the study area, the Abbassabad Syncline (ABS) has folded the Fajan and Karaj Formations (station 13 in Fig. 6). It is an open and gently plunging upright fold with a subvertical NE-SW-trending axial plane.

The Mesozoic succession is also intensely folded in the central parts of the study area. For instance, the Kelyab and Kuhe-e-Chenaran Anticlines are NE-SW-trending folds that are moderately plunging to the WSW and unconformably covered by the Fajan Formation. They seem to be associated with the high-angle reverse faults further northeast. In the hanging wall of the DF, the Diktash Anticline (DA) is and upright anticline whose axis gently plunges to the southwest (Fig. 11b; station 31 in Fig. 6).

Abundant folds have developed in southwestern parts of the area (Salamati, 2013). They are large wave-length folds that have deformed middle Eocene to Pliocene deposits. For example, the Eskadar Anticline (station 19 in Fig. 12) is an open fold with a horizontal axis and a subvertical axial plane. The core of the Eskadar anticline is truncated by minor faults that cut across southern side of the valley.

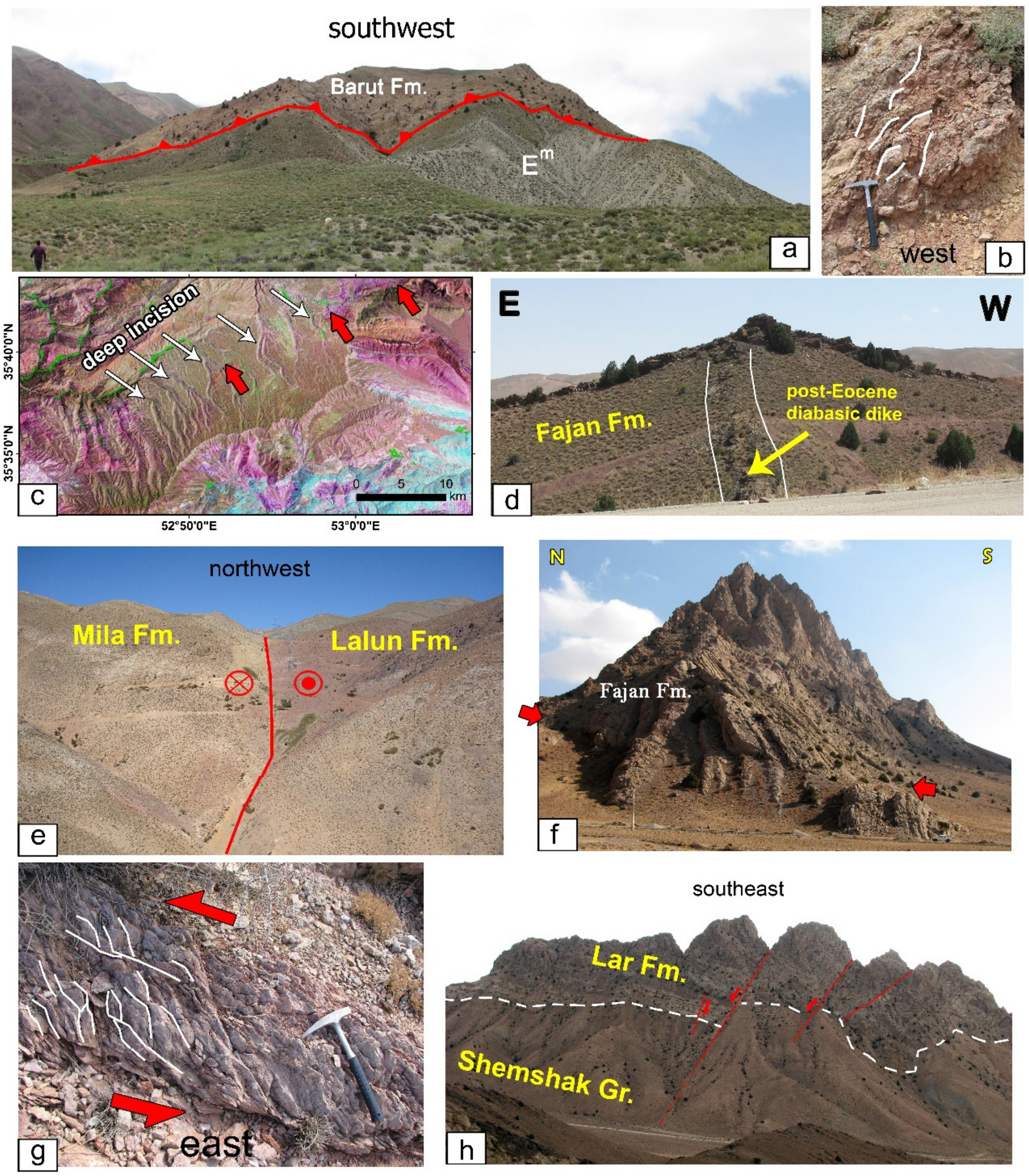

Figure 9. (a) In the central-eastern parts (station 4) the BF thrusts the Early Cambrian Barut, Zagun and Lalun Formation over the middle Eocene marl, sandstone and tuff (E^m). (b) Fairly sigmoidal shear planes in the fault zone of BF at (a). (c) Deeply incised Plio-Quaternary deposits in the western end of BF. Red and white arrows show fault trace and deep incisions, respectively. (d) A diabasic dike exposed within the Fajan Formation. (e) A right-lateral fault affecting the lower Paleozoic formations in the north of the study area. (f) A left-lateral minor transversal fault with (g) well-developed shear planes. (h) The normal faults cross the Lar Formation in the northern parts of the study area

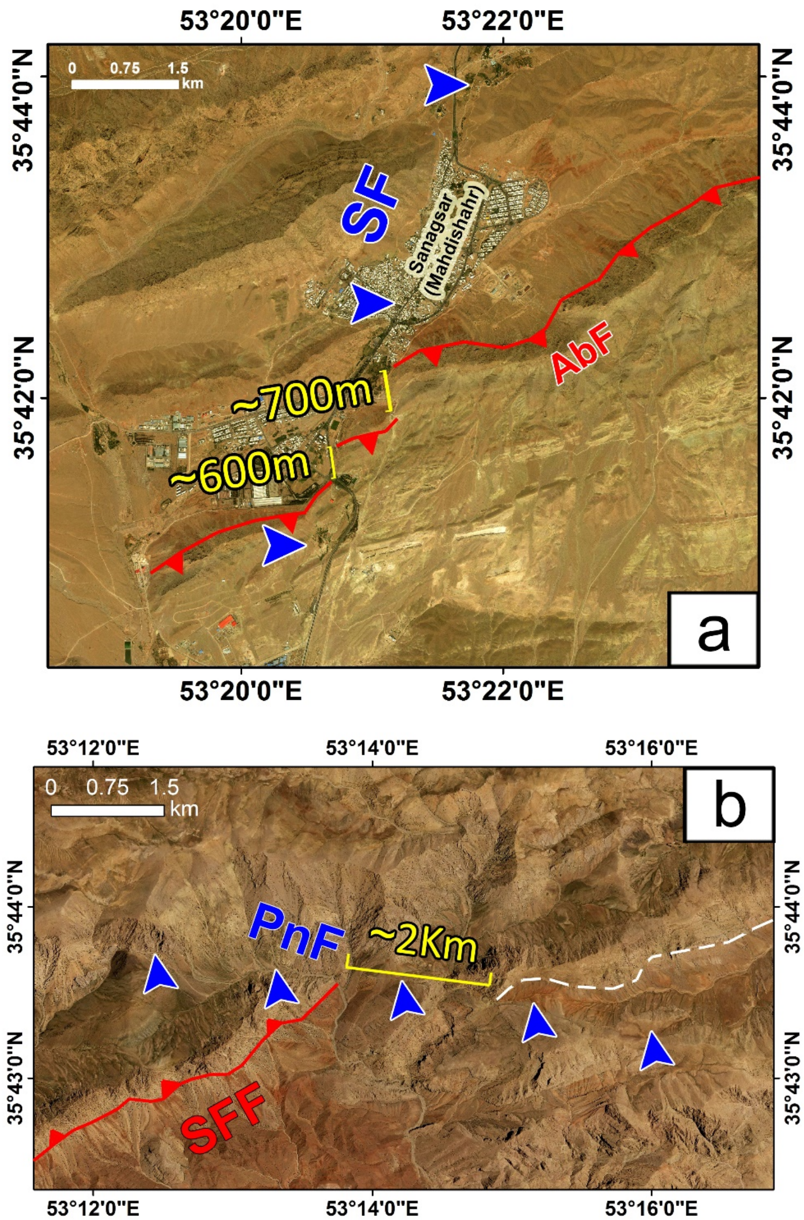

Figure 10. (a) The SF is a left-lateral transversal fault that has displaced other major faults. (b) The base of the Fajan Formation (white dashed lines) has been offset by ~2km by the PnF

The Golroo Anticline (station 20 in Fig. 12) is another anticline with a similar geometry and an axis slightly plunging to NE. Several smaller scale folds (e.g., Kuh-e-Sefid Synclinh; station 18 in Fig. 12) have developed in the northern limb of the Golroo anticline. The Kuh-e-Sorkhi Syncline is cored by Pliocene terrestrial deposits ($Pl^{c,m,s}$) that unconformably overlie the Miocene and older formations. To the east, the Kuh-e-Gachi Syncline (station 11 in Fig. 12) is an upright fold exposing the Oligocene and Miocene formations in the core.

Within the core of the Cheshmeh Shirin Anticline (station 17 in Fig. 12) lies a ~10 km-long, ~2 km-wide deep valley incised through the anticline, demonstrating existence of high proportion of erodible material contained within the middle to upper Eocene units. The southern limb of the Golroo Anticline turns into smaller scale Siyahsuk Anticline (Fig. 11c) (station 21 in Fig. 12) that is an upright fold whose axis gently plunges to the northeast. There are some parasitic folds in the hinge zone of this fold. For instance, Fig. (11d) shows a Z-shaped minor fold in which layers slipped upon one another. Slickenlines developed on bedding planes (Fig. 11e) suggest that the anticline responded to the shortening via a flexural slip mechanism, involving simple shear across bedding planes (e. g., Ramsay & Huber, 1983). To the south, the Namakdan Anticline (NA) (station 22 in Fig. 12) has deformed the Oligocene and Miocene formations is the youngest and southernmost fold developed in this area in relation to the NF (Figs. 7c and 11f). Gypsum layers of the EO^g that cover much of the southwest of the study area have been folded extensively and they occur in the cores of many synclines (Fig. 11g).

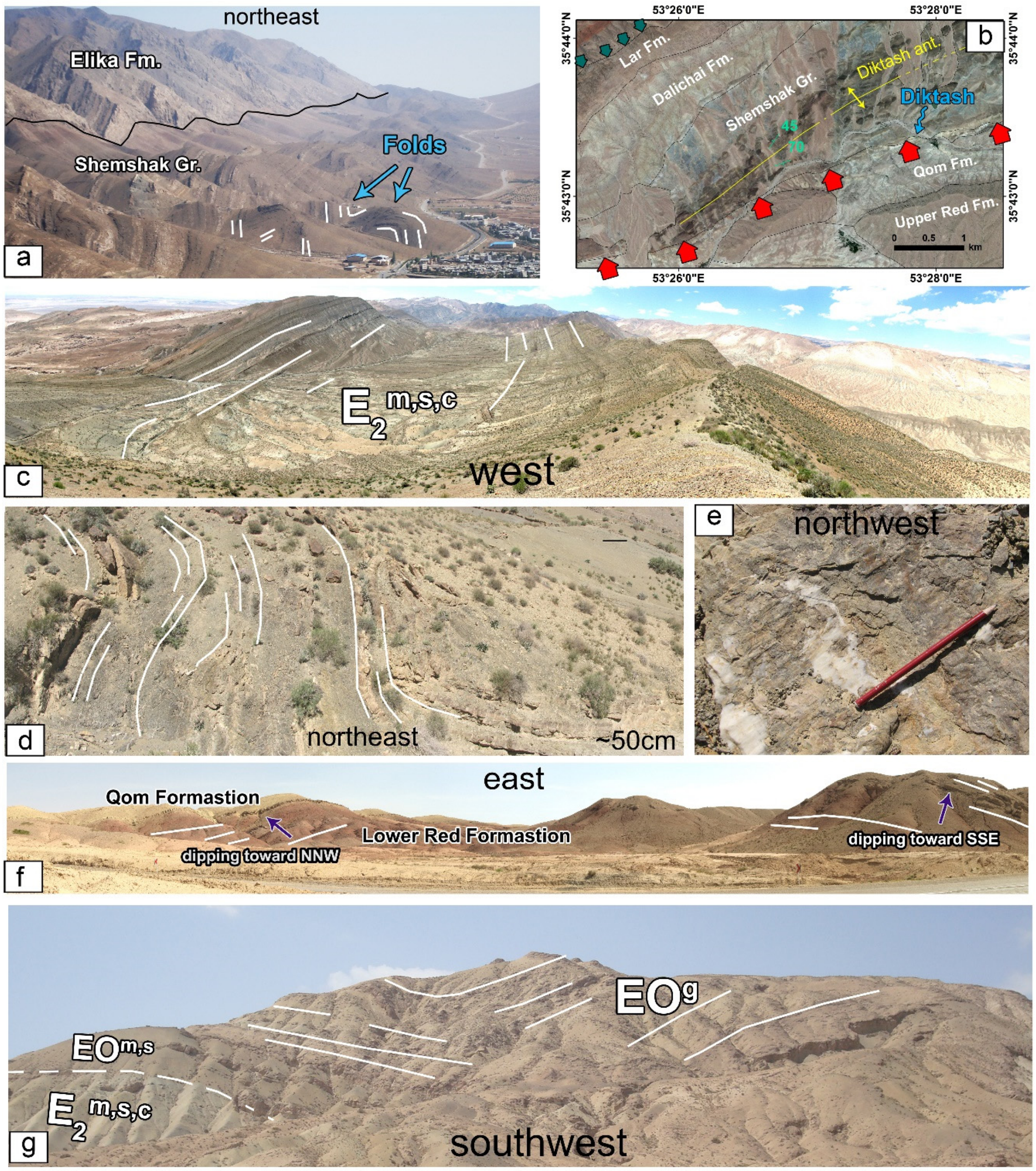

Figure 11. (a) Several folds developed in the Shemshak Group to the north of the city of Shahmirzad. (b) The Diktash Anticline is an upright fold related to the DF (red arrows). The Green arrows mark the trace of the AbF. (c) The Siyahsuk Anticline in the southwest of the study area. (d) A Z-shaped parasitic fold formed by layers dragged in the hinge zone of the Siyahsuk Anticline. (e) The reverse-slip slickenlines on the layers of the Siyahsuk Anticline. (f) The Namakdan Anticline in the SW of the study area. (g) An open syncline developed in the upper Eocene-Oligocene marl and gypsum (EO^g) (Salamati, 2013)

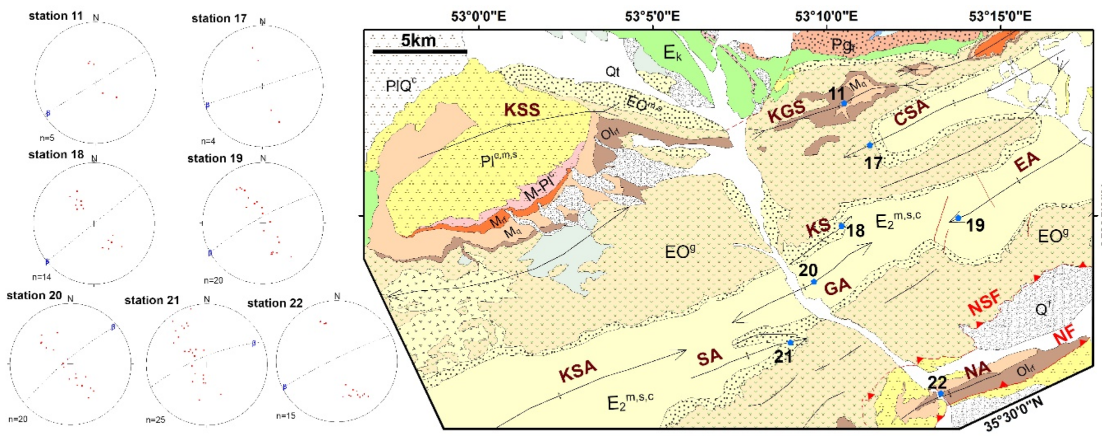

Figure 12. A simplified geological map showing the folds devolved in southwest of the study area. The measurement stations are indicated as blue pentagonals and black bold numbers. Stereonet plots are provided for each station. Abbreviations: CSA: Cheshmeh Shirin Anticline; EA: Eskadar Anticline; GA: Golroo Anticline; KS: Kuh-e-Sefid Syncline; KGS: Kuh -e- Gachi Syncline; KSA: Kuhe-e-Sangtarashan Anticline; KSS: Kuh -e- Sorkhy Syncline; NA: Namakdan Anticline; NF: Namakdan Fault; NSF: North Semnan Fault; SA: Siyahsuk Anticline. The legend is the same as the one in Figs. 2 and 6

Discussion

Geometry and kinematics of the structures

Our structural investigations revealed that in the SE Alborz Mountains deformation style varies from thrust loading plus dominant folding in the southwest to high-angle reverse faulting in the northeast. This is best indicated by the cross sections (Fig. 3). In the southwest, development of numerous folds characterizes a "fold belt" compatible with a thin-skinned deformation style (se e.g., Alavi, 1996; Guest et al., 2006a). Alavi (1996) suggested that folds in Alborz Mountains are mostly fault-related and disharmonic. Yet, folds in the southwest of the study area are of simple geometries i.e. mainly upright and open with vertical to steeply-inclined axial surfaces and axes plunging either to the NE or SW. The NSF is bordering the range and responsible for thrust loading in this part of the SE Alborz Mountains. The NF is medium-angle and accommodates progression of deformation front to the southeast.

Some folds might have formed as a result of a "flexural slip" mechanism. This is most evident where slickenlines and parasitic folds are observed in the hinge zone of the folds (e. g., Siyahsuk anticline) (Figs. 11d and e). However, where mainly the marl and gypsum layers have been folded (Fig. 11g), other mechanisms may have played a part (e. g., Ramsay & Huber, 1983; Davis & Engelder, 1985). Generally, evaporites involved in deformation may have acted as detachment levels in the southern Alborz Mountains (Allen et al., 2003). Using 2D seismic data, Bouzari et al, (2013) reported the existence of two detachment horizons in the LRF and URF further southeast in the foreland basin. However, subsurface data are required to prove whether this might also be the case in the study area. Existence of a thick succession of middle Eocene to Miocene and even Pliocene shale, siltstone, mudstone and marl (Fig. 5), regarded as incompetent materials, as well as huge volumes of upper Eocene-lower Oligocene gypsum facilitated folding in the southwest of the study area. However, to the northeast, where this succession is thinner, high-angle reverse faults occur that strike NE-SW in agreement with the general trend of eastern arm of the Alborz Mountains. The DF, AnF, AbF and BF do not continue very long to the southwest and are associated with anticlines in their western tips. It is likely that they have not emerged in the southwest and contributed to creation of some anticlines (e.g., Kelyab and Kuhe-e-Chenaran Anticlines). In the northeast of the study area, fold are expected to be tighter and show inclined axial planes, however, they maintain rather similar geometries to the ones in the southwest (ABS at station 13). Consequently, the thickness of rock units within the SE Alborz sedimentary basin during the late Cenozoic played a crucial role in the variations of the deformation style. Other significant deformational differences are in the hanging wall of the high-angle faults e.g., BF, PF and AnF where considerable titling, uplift, fracturing and minor faulting occurred in contrast to areas covered by Neogene units where mostly fold and less number of faults are present (see cross sections in Fig. 3).

Regional kinematics

Kinematic complexities are observed in different parts of the Alborz Mountains (see e.g., Yassaghi & Madaipour, 2008; Yassaghi & Naeimi, 2011). A variety of senses of slip are observed along the major faults in the study area (Fig. 6). However, oblique-slip shear planes are very common in the SE Alborz Mountains, suggesting that the compression direction was not perpendicular to the trend of the faults at the time. The trend of post-Eocene dikes (station 29) in the SE Alborz Mountains are compatible with a ~ NNW-oriented compression that is not consistent with the current north-northeastward direction of strain (Nemati et al., 2013; Khorrami et al., 2019). Consequently, a change in the compression direction or structural trends could have occurred since these structures formed. A poorly dated change from NW- to a NE-oriented shortening have been suggested by several researchers in the Alborz Mountains (Axen et al., 2001; Zanchi et al., 2006; Guest et al., 2006a; Landgraf et al., 2009; Ballato et al., 2011). Axen et al., (2001) proposed that this changeover occurred before ~ 8–6Ma. This older NW-oriented shortening regime must have been active prior to ~ 9Ma (Ballato et al., 2011) or ~ 18 Ma (Ballato et al., 2013). Since the AnF, AbF and DF are cut by the transversal faults such an NW-oriented shortening could have lasted until Plio-Quaternary times. Recently, Mattei et al., (2017, 2019) suggested vertical-axis-rotations and oroclinal bending in the Alborz Mountains. Mattei et al., (2019) suggested that the onset of the oroclinal bending processes occurred about 6–4 myr ago and they are no longer active. They concluded that the present-day kinematics of northern Iran is not older than ~2 Ma. This possibly explains why the present-day shortening direction is at odd with the inferred paleostress directions (Shahidi, 2008). Further west, post-Eocene vertical-axis-rotations were suggested by Rezaeian et al., (2020) to have also occurred in the Talesh Mountains. The obliquely oriented folds in the footwall of the PF and DF indicate a post-Miocene left-lateral transpression in the southeast of the study area.

Tectonic evolution of the SE Alborz Mountains during the late Cenozoic

In this area, the Paleocene (?) to Eocene Fajan Formation is unconformablely lying upon the deformed lower Paleozoic-Mesozoic formations. The irregular outcrop pattern of this formation exhibits that it has filled a rugged topography resulted from the Late Cretaceous-early Paleocene compressional events. Upon that, lies the middle Eocene Karaj Formation. According to the literature (see e.g., Brunet et al., 2003; Shahidi, 2008; Verdel et al., 2011; Javadi et al., 2020; Shafiei Bafti et al., 2021) the southern Alborz Mountains basins underwent a middle (?) Eocene extensional phase of subsidence (stage a in Fig. 13) accompanied by volcanism. There are a number of local angular unconformities within the middle Eocene-Pliocene succession, indicating tectonic instabilities of the SE Alborz Mountains during the late Eocene - early Oligocene times. These instabilities followed the onset of reverse activity on the BF, AnF and AbF and creation of folds e.g., in their tips or hanging wall areas (stage b in Fig. 13). This also led to folding of the Karaj and older formations plus uplift of the SE Alborz Mountains and establishment of a shallow-water marine basin suited for deposition of the middle-upper Eocene-lower Oligocene marl and evaporitic units.

Naeimi et al., (2022) suggested that the foreland basin could have begun to develop in the early Miocene shortly after the onset of reverse activity on the NSF (stage c in Fig. 13). The coarse-grained Pliocene deposits unconformably overlay the folded upper Eocene-Miocene succession (stage d in Fig. 13). Rieben (1955) suggested that the elevation of the Alborz Mountains was renewed in late Pliocene or early Quaternary. We suggest that the DF began to thrust Mesozoic rock units upon the upper Eocene-Miocene deposits sometime between the middle Miocene to the latest Pliocene-Quaternary (stage d in Fig. 13). To the northeast, the fault has affected the Pliocene rocks and is covered by the Plio-Quaternary clastic deposits. In the southwest, the Pliocene deposits are folded and cut by the NF, indicating that deformation is advancing to the south and range continued to grow after the Pliocene (stage e in Fig. 13). The creation of the PF as a back thrust followed the thrusting of the SE Alborz Mountains upon the foreland (i.e. the NE Central Basin) sometime between the middle Miocene to the latest Pliocene-Quaternary times. Because the AnF, AbF and DF are truncated by the transversal faults the above mentioned NW-oriented compression could have lasted until Plio-Quaternary times. All of these are synchronous with the late Miocene to Pliocene pulse of fast exhumation in the Alborz Mountains (Rezaeian et al., 2012; Ballato et al., 2013). The foreland of the SE Alborz Mountains was disrupted in the latest Pliocene-Quaternary times due to reverse reactivation of the pre-existing Attary Fault as a result of Arabia-Eurasia collision and the regional kinematic changes in the South Caspian Basin (Naeimi et al., 2022). We suggest that a significant episode of deformation took place during late Miocene-late Pliocene evidenced by angular unconformities and onset of reverse activity on the faults like PF and DF. At the present, a complicated pattern of outcrops are observed (stage f in Fig. 13) that resulted from formation or reactivation of several fault during the late Cenozoic.

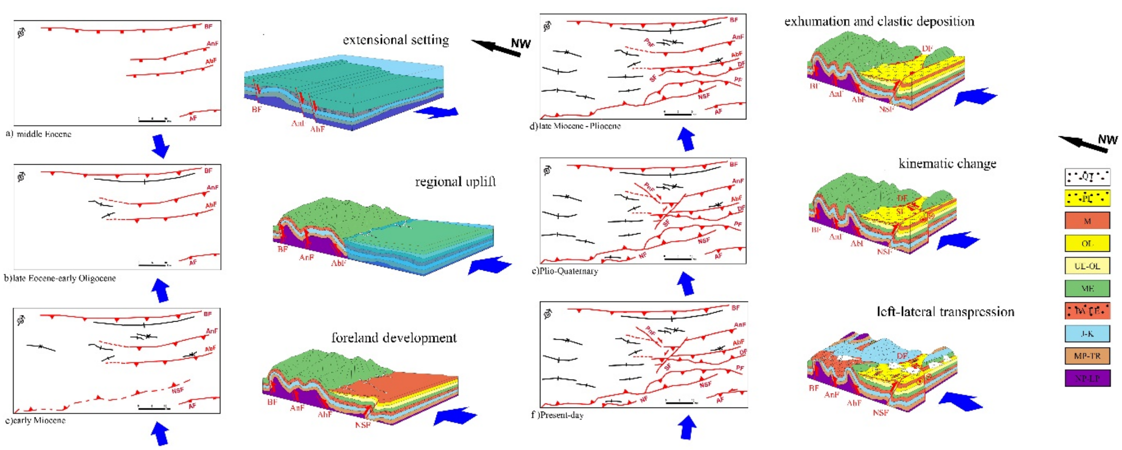

Figure 13. Schematic 2D and 3D diagrams showing the evolution scenario of the SE Alborz Mountains during the late Cenozoic. (a) During the middle Eocene the Karaj Formation was being deposited in an extensional setting on the Fajan Formation which had rested unconformably upon the folded Paleozoic-Mesozoic succession. (b) From the late Eocene to Oligocene the area began to rise due to onset of (or reactivation?) reverse kinematics on the BF, AnF and AbF and regional uplift. (c) In the early-middle Miocene the foreland started to develop and thrust loading initiated via the incipient NSF. (d) In the late Miocene-Pliocene clastic materials shed to the area over the older units. The PF and DF formed sometime between the middle Miocene to the latest Pliocene-Quaternary. (e) The NW-oriented shortening could have lasted until Plio-Quaternary times. (f) After erosional removals, a rather complicated pattern of outcrops are observed with a present-day left-lateral pattern of the deformation. Abbreviations in the legend are: NP-LP: Neoproterozoic-lower Paleozoic units; MP-TR: middle Paleozoic -Triassic succession; J-K; Jurassic and Cretaceous Formations; PA-LE: Paleocene-lower Eocene formations; ME: middle Eocene volcanicalstic and detrital rocks; UE-OL: upper Eocene marl and evaporitic rocks; OL: Oligocene LRF; M: Miocene QF and URF; PL: Pliocene clastic materials transported from growing elevations; QT: Quaternary deposits

The growth of the eastern Central Alborz Mountains

As it was mentioned above, there is a varied range of evidence indicating that the southern Alborz Mountains have undergone a regional extensional setting during the middle (?) Eocene (see e.g., Brunet et al., 2003; Shahidi, 2008; Verdel et al., 2011). Consequently, it can be inferred that the late Eocene-early Oligocene reverse kinematics on the southward-dipping high-angle faults e.g. BF may demonstrate a kinematic reversal event following a rather prolonged period of tensional kinematics. The reactivation of major faults of the Central Alborz Mountains was reported by many authors (see e.g., Yassaghi, 2005; Nazari, 2006; Zanchi et al., 2006; Ehteshami Moinabadi & Yassaghi, 2007; Yassaghi & Madanipour, 2008; Yassaghi & Naeimi, 2011, Javadi et al., 2020). In contrast to the range-front thrust or reverse faults (Fig. 1) (e.g., the Khazar, Garmsar, North Semnan and North Damghan faults) that dip inward the Eastern Alborz Mountains range, the major faults inside the belt (e.g., Chashm, Bashm, Mosha faults) dip to either sides of the range and do not follow a systematic pattern of thrusting in contrast to typical fold-and-thrust belts (see e.g. Marshak & Wilkerson, 2004; Poblet & Lisle, 2011). Thrust stacking (Aalvi, 1996) or back thrust faulting (Yassaghi, 2005) have been put forward to explain this. It can be inferred that despite the outward growth of the range since the late Cenozoic (Ballato et al., 2011; Rezaeian et al., 2012; Saberi et al., 2018), it is also possible that the amplification of the inner eastern Central Alborz Mountains is a product of fault kinematic reversals and inversion of subbasins (e.g., footwall of the BF) that have been repeatedly extended or contracted since the Mesozoic (Shahidi, 2008; Javadi et al., 2020). Outward propagation of the thrust or reverse faults (e.g., NSF and KHF) contributed to the growth of the eastern Central Alborz range (Ballato et al., 2008). Additionally, the left-lateral Shahrud Fault System has also played a significant role in accommodation of the present-day deformation in the Eastern-Central Alborz Mountains (Nemati et al., 2011).

Insights into the Arabia-Eurasia continental collision

Several studies have suggested that the Arabia-Eurasia collision initiated in latest Eocene to early Oligocene times (e.g., see e.g. Ballato et al., 2011 and the references therein). For instance, Allen & Armstrong (2008) reviewed the supporting evidence in this respect including compressional deformation, major surface uplift, exhumation, non-deposition or angular unconformities, onset of terrestrial sedimentation, changes in palaeobio- geography, the switch-off of arc magmatism. They suggested the closure of the Tethys ocean gateway at ~35 Ma to be marking the initial collision. However, it has recently been suggested that continental collision between Arabia and Eurasia did not initiate until ~27 Ma (McQuarrie & van Hinsbergen, 2013) or ~26 Ma (Koshnaw et al., 2018) in the late Oligocene time. There seems to be lag time between ~ 35 to 27Ma.

In the study area, the middle Eocene to Miocene succession is limited to the southeastern third of the study area, which indicates that the rest of the region had already been uplifted by the latest Eocene-Oligocene time. The reverse kinematics on BF, AnF and AbF are accompanied by folding in their tips. A drastic reverse kinematics on the BF caused the area to rise since no major Oligocene deposits has been reported in the footwall of this fault (stage b in Fig. 13) (Nabavi, 1987). Deposition of a ~100m- thick upper Eocene-early Oligocene marl and gypsum-bearing unit in the SE Alborz Mountains followed this event. A late Eocene contractional deformation has been also detected through low-temperature thermochronometric studies (Rezaeian et al., 2012). Further north, the red conglomerate proceeded by marl and gypsum indicate this isolation during the late Eocene transition (Naeimi & Shiri Jian, 2021). This late Eocene-Oligocene compression is generally attributed to the onset of the Arabia-Eurasia collision (Brunet et al., 2003; Shahidi, 2008; Ballato et al., 2011; Rezaeian et al., 2012).

In the SE Alborz Mountains, the QF is early Miocene in age (Nabavi, 1987; Alavi-Naini 1997: Naeimi & Shiri Jian 2021). This formation is in turn overlain by basal conglomerates and continental red clastic rocks of the URF above an erosional unconformity that marks the emergence and subaerial exposure of the Alborz Mountains region (Rezaeian et al., 2012). Thermochronologic data also revealed an acceleration of uplift and exhumation in the early to late Miocene (see e.g. Ballato et al., 2011 for a detailed review and for the references therein). This led Ballato et al., (2011) to propose a two-stage collision process including a "soft collision" (subduction of the stretched continental Arabian lithosphere beneath Eurasia) and a "hard collision" (arrival of buoyant Arabian lithosphere in the subduction zone). Based on the field investigations and low-temperature thermochronology, Tadayon et al., (2018) suggested the full mechanical coupling between the Zagros convergence zone (in the southwest of Iran) and its hinterland domain (central Iran) took place in 40–35 Ma, during the late Eocene-early Oligocene. Our data suggest the late Eocene-early Oligocene as the onset of the initial collision of the Arabian and Eurasian Plates. We propose that the unconformity and red conglomerate above and below the QF represent later stages of Arabia-Eurasia collision as Ballato et al., (2011) suggested.

Conclusions

Deformation style varies within the SE Alborz Mountains from large wave-length folding in the southwest to high-angle reverse faulting in the northeast due to existence of incompetent units. The incompetent units were deposited in a shallow-water marine basin that came to existence as a consequence of onset of reverse kinematics (or kinematic reversal?) on the BF in the late Eocene. Such a change is conventionally attributed to the onset of collision between the Arabia and Eurasia Plates resulting. Our data also revealed that the late Miocene-late Pliocene was a critical period when regional surface uplift took place and substantial clastic materials were shed upon the already folded rock units. In the SE Alborz Mountains the high-angle reverse faults have strike-slip shear planes as well, indicating the compression direction was not perpendicular to the trend of the faults at the time. The contractional and transversal structures plus the post-Eocene dikes in the SE Alborz Mountains are consistent with an N to NW-oriented compression that does not agree with the present-day north-northeastward direction of the strain. Consequently, a change in the shortening direction or counter clockwise vertical-axis-rotation of the structures seem to have occurred since the faults formed.

Acknowledgements

This paper is part of the first author's Ph.D. dissertation at Shahid Beheshti University. The Geological Survey of Iran and Shahid Beheshti University are acknowledged for providing logistic and analytical support. Authors also benefited from constructive discussions with M.R. Ghassemi, P. Ballato. H. R. Javadi and H. Nazari. The Editor-in Chief and two reviewers are appreciated for their constructive comments that improved the manuscript.

References

Aghanabati, S. A., Hamedi, A. R., 1994. Geological map of Semnan quadrangle scale 1:250000. Geological Survey of Iran, Tehran, Iran.

Aghanabati, A., 2004. Geology of Iran. Geological Survey of Iran, Tehran, Iran, 620p. (In Persian).

Alavi, M., 1996. Tectonostratigraphic synthesis and structural style of the Alborz Mountain System in Iran. Journal of Geodynamics 21: 1-33.

Alavi-Naini, M., 1972. Etude geologique de la region de Djam. Geological Survey of Iran, Tehran, Iran. Report no. 23: 288p.

Alavi-Naini, M., 1997. Geological map of Jam Quadrangle Scale 1:100000. Geological Survey of Iran, Tehran, Iran.

Allen, M. B., Ghassemi, M. R., Shahrabi, M., Qorashib, M., 2003. Accommodation of late Cenozoic oblique shortening in the Alborz range, northern Iran. Journal of Structural Geology 25: 659-672.

Allen, M.B., Armstrong, H.A., 2008. Arabia-Eurasia collision and the forcing of mid-Cenozoic global cooling: Palaeogeography, Palaeoclimatology, Palaeoecology 265: 52-58.

Amini, A., 1997. Provenance and depositional environment of the Upper Red Formation, Central Zone, Iran. (Ph.D. thesis). Manchester University, 320p.

Angiolini, L., Gaetani, M., Muttoni, G., Stephenson, M. H., Zanchi, A. 2007. Tethyan oceanic currents and climate gradients 300 m.y. ago. Geology 35: 1071–1074.

Assereto, R., 1966. The Jurassic Shemshak Formation in central Elburz (Iran): Reviews in Italian Paleontology and Stratigraphy 72: 1133-1182.

Axen, G. J., Lam, P. S., Grove, M., Stockli, D. F., Hassanzadeh, J., 2001. Exhumation of the west-central Alborz Mountains, Iran, Caspian subsidence, and collision-related tectonics. Geology 29: 559-562.

Ballato, P., Nowaczyk, N. R., Landgraf, A., Strecker, M. R., Friedrich, A., Tabatabaei, S. H., 2008. Tectonic control on sedimentary facies pattern and sediment accumulation rates in the Miocene foreland basin of the southern Alborz Mountains, northern Iran. Tectonics 27: 1-20.

Ballato, P., Uba, C. E., Landgraf, A., Strecker, M. R., Sudo, M., Stockli, D. F., Friedrich, A., Tabatabaei, S. H., 2011. Arabia-Eurasia continental collision: Insights from late Tertiary foreland-basin evolution in the Alborz Mountains, northern Iran. GSA Bulletin 123: 106-131.

Ballato, P., Stockli, D.F., Ghassemi, M.R., Landgraf , A., Strecker, M.R., Hassanzadeh, J., Friedrich, A., Tabatabei, S. H., 2013. Accommodation of transpressional strain in the Arabia–Eurasia collision zone: new constraints from (U–Th)/He ther-mochronology in the Alborz Mountains, N Iran. Tectonics 32, TC003159.

Ballato, P., Landgraf, A., Schildgen, T. F., Stockli, D. F., Fox, M., Ghassemi, M. R., Kirby, E., Strecker, M. R., 2015. The growth of a mountain belt forced by base-level fall: Tectonics and surface processes during the evolution of the Alborz Mountains, N Iran. Earth and Planetary Science Letters 425: 204–218.

Balling, P., Tomljenović, B., Schmid, S. T., Ustaszewski, K., 2021. Contrasting along-strike deformation styles in the central external Dinarides assessed by balanced cross-sections: Implications for the tectonic evolution of its Paleogene flexural foreland basin system. Global and Planetary Change.

Berberian, M., King, G. C., 1981. Towards a palaeogeography and tectonics evolution of Iran. Canadian Journal of Earth Science 18: 210-265.

Berberian, M., Qorashi, M., Shoja-Taheri, J., Talebian, M., 1996. Seismotectonic earthquake-fault hazard investigations in the Semnan region. Contribution to Seismotectonics of Iran, Part VII. Geological Survey of Iran. Report no. 63: 277p. (In Persian).

Berberian, M., Walker, R. T., 2010. The Rudbar Mw 7.3 earthquake of June 20 1990: Seismotectonics, coseismic and geomorphic displacements, and historic earthquakes of the western 'High-Alborz', Iran. Geophysical Journal International 182: 1577-1602.

Bouzari, S., Konon, A., Koprianiuk, M., Julapour, A. A., 2013. Thin-skinned tectonics in the Central Basin of the Iranian Plateau in the Semnan area, Central Iran. Journal of Asian Earth Sciences 62: 269-281.

Bozorgnia, F., 1966. Qum formation stratigraphy of the Central Basin of Iran and its intercontinental position. Bulletin of Iranian Petroleum Institute 24: 69-76.

Brunet, M.-F., Korotaev, M. V., Ershov, A.V., Nikishin, A. M., 2003. The South Caspian Basin: a review of its evolution from subsidence modeling. Sedimentary Geology 156: 119-148.

Davis, D. M., Engelder, T., 1985. The role of salt in fold-and-thrust belts. Tectonophysics 119: 67-88.

Djamour, Y., Vernant, P., Bayer, R., Nankali, H. R., Ritz, J.-F., Hinderer, J., Hatam, Y., Luck, B., Le Moigne, N., Sedighi, M., Khorrami, F., 2010. GPS and gravity constraints on continental deformation in the Alborz Mountain range, Iran. Geophysical Journal International 183: 1287–1301.

Ehteshami Moinabadi, E. M., Yassaghi, A., 2007. Geometry and kinematics of the Mosha Fault, south central Alborz Range, Iran: An example of basement involved thrusting. Journal of Asian Earth Sciences 29: 928-938.

Ehteshami-Moinabadi, M., 2014. Fault zone migration by footwall shortcut and recumbent folding along an inverted fault: example from the Mosha Fault, Central Alborz, Northern Iran. Canadian Journal of Earth Sciences 51: 825- 836.

Fürsich, F.T., Wilmsen, M., Seyed-Emami, K., Majidifard, M.R., 2009a. Lithostratigraphy of the Upper Triassic-Middle Jurassic Shemshak Group of Northern Iran. In: Brunet, M.-F., Wilmsen, M., Granath, J. W. (Eds.), South Caspian to Central Iran Basins. The Geological Society, London, Special Publications 312, pp. 120-169.

Fürsich, F. T., Wilmsen, M., Seyed-Emami, K., Majidifard, M. R., 2009b. The Mid-Cimmerian tectonic event (Bajocian) in the Alborz Mountains, northern Iran: Evidence of the break-up unconformity of the South Caspian Basin, In: Brunet, M.-F., Wilmsen, M., Granath, J. W. (Eds.), South Caspian to Central Iran Basins. The Geological Society, London, Special Publications 312: 189-203.

Ghassemi, M. R., 2005. Drainage evolution in response to fold growth in the hanging-wall of the Khazar Fault, north-eastern Alborz, Iran. Basin Resarch 17: 425-436.

Giambiagi, L., Mescua, J., Bechis, F., Tassara, A., Hoke, G., 2012. Thrust belts of the southern Central Andes: Along-strike variations in shortening, topography, crustal geometry, and denudation. GSA Bulletin 124: 1339-1351.

Geyer, G., Bayet-Goll, A., Wilmsen, M., Mahboubi, A., Moussavi-Harami, R., 2014. Lithostratigraphic revision of the middle Cambrian(Series 3) and upper Cambrian (Furongian)in northern and central Iran. Newsletters on Stratigraphy 47: 21-59.

Guest, B., Axen, G. J., Lam, P.S., Hassanzadeh, J., 2006a. Late Cenozoic shortening in the west-central Alborz Mountains, northern Iran, by combined conjugate strike-slip and thin-skinned deformation. Geosphere 2: 35-52.

Guest, B., Stockli, D. F., Grove, M., Axen, G. J., Lam, P. S., Hassanzadeh, J., 2006b. Thermal histories from the central Alborz Mountains, northern Iran: Implications for the spatial and temporal distribution of deformation in northern Iran. Geological Society of America Bulletin 118: 1507-1521.

Guest, B., Horton, B. K., Axen, G. J., Hassanzadeh, J., McIntosh, W. C., 2007. Middle to late Cenozoic basin evolution in the western Alborz Mountains: Implications for the onset of collisional deformation in northern Iran. Tectonics 26: 1-26.

Gwinn, V. E., 1964. Thin-skinned tectonics in the plateau and northwestern Valley and Ridge provinces of the Central Appalachians. Bulletin of the Geological Society of America 75: 863–900.

Hollingsworth, J., Jackson, J., Walker, R., Gheitanchi, M.R., Bolourchi, M.J., 2006. Strike-slip faulting, rotation and along-strike elongation in the Kopeh Dagh Mountains, NE Iran. Geophysical Journal International 166: 1161-1177.

Hollingsworth, J., Nazari, H., Ritz, J.-F., Salamati, R., Talebian, M., Bahroudi, A., Walker, R. T., Rizza, M., Jackson, J., 2010. Active tectonics of the east Alborz mountains, NE Iran: Rupture of the left-lateral Astaneh fault system during the great 856 A.D. Qumis earthquake. Journal of Geophysical Research 115: B12313.

Jackson, J., Priestley, K., Allen, M. B., Berberian, M., 2002. Active tectonics of the South Caspian Basin. Geophysical Journal International 148: 214-245.Javadi, H. R., Kouhpeyma, M., Gholami Zadeh, P., Naeimi, A., Sheikholeslami, M. R., Ghassemi, M. R., 2020. Deploying depositional and stratigraphic evidence in kinematic investigations along multi-role faults: The case study from the eastern Mosha Fault, central Alborz Range, northern Iran. Journal of Asian Earth Sciences 187.

Julivert, M., Arboleya, M. L. 1984. A geometrical and kinematical approach to the nappe structure in an arcuate fold belt: the Cantabrian nappes (Hercynian chain, NW Spain). Journal of Structural Geology 6: 499-519.

Khorrami, F., Vernant, P., Masson, F., Nilfouroushan, F., Mousavi, Z., Nankali, H., Saadat, S. A., Walpersdorf, A., Hosseini, S., Tavakoli, P., Aghamohammadi, A., Alijanzade, M., 2019. An up-to-date crustal deformation map of Iran using integrated campaign-mode and permanent GPS velocities. Geophysical Journal International 217: 832-843.

Koshnaw, R.I., Stockli, D.F., and Schlunegger, F., 2018. Timing of the Arabia-Eurasia continental collision—Evidence from detrital zircon U-Pb geochronology of the Red Bed Series strata of the northwest Zagros hinterland, Kurdistan region of Iraq. Geology 47: 47-50.

Landgraf, A., Ballato, P., Strecker, M. R., Friedrich, A., Tabatabaei, S. H. and Shahpasandzadeh, M., 2009. Fault-kinematic and geomorphic observations along the North Tehran Thrust andMosha Fasham Fault, Alborz mountains Iran: implications for fault-system evolution and interaction in a changing tectonic regime. Geophysical Journal International 177: 676-690.

Madanipour, S., Ehlers, T.A., Yassaghi, A., Enkelmann, E., 2017. Accelerated middle Miocene exhumation of the Talesh Mountains constrained by U-Th/He thermochronometry: Evidence for the Arabia- Eurasia in the NW Iranian Plateau. Tectonics 36: 1538-1561.

Mattei, M., Cifelli, F., Alimohammadian, A., Rashid, H., Winkler, A., Sagnotti, L., 2017. Oroclinal bending in the Alborz Mountains (Northern Iran): New constraints on the age of South Caspian subduction and extrusion tectonics. Gondwana Research 42: 13-28.

Mattei, M., Visconti, A. L., Cifelli, F., Nozaem, R., Winkler, A., Sagnotti, L., 2019. Clockwise paleomagnetic rotations in northeastern Iran: Major implications on recent geodynamic evolution of outer sectors of the Arabia-Eurasia collision zone. Gondwana Research 71: 194-209.

Marshak, S., Wilkerson, M. S., 2004. Fold-thrust belts. In: van der Pluijm B. A. and Marshak, S. (Eds), Earth structure: an introduction to structural geology and tectonics. 2nd edition. W. W. Norton & Company, Inc. pp.444-474.

McQuarrie, N., van Hinsbergen, D. J. J., 2013. Retrodeforming the Arabia-Eurasia collision zone: Age of collision versus magnitude of continental subduction. Geology 41: 315-318. -

Muttoni, G., Mattei, M., Balini, M., Zanchi, A., Gaetani, M., Berra, F. 2009a. The drift history of Iran from the Ordovician to the Triassic, In: Brunet, M.-F., Wilmsen, M., Granath, J. W. (Eds.), South Caspian to Central Iran Basins. The Geological Society, London, Special Publications 312: 7-29.

Muttoni, G., Gaetani, M., Kent, D.V., Sciunnach, D., Angiolini, L., Berra, F., Garzanti, E., Mattei, M., Zanchi, A., 2009b. Opening of the Neo-Tethys Ocean and the Pangea B to Pangea A transformation during the Permian. GeoArabia 14: 17-48.

Nabavi, M. H., 1987. Geological map of Semnan Quadrangle Scale 1:100,000. Geological Survey of Iran.

Naeimi, A., Shiri Jian, A., 2021. Geological map of Sefidargoleh Quadrangle Scale 1:50000. Geological Survey of Iran, Tehran, Iran. (Under review).

Naeimi, A., Alavi , S. A., Madanipour, S., 2022. Tectonic evolution of foreland basin of the SE Alborz Mountains, northern Iran. Journal of Asian Earth sciences, 104981.

Nazari, H., 2006. Analyse de la tectonique recente et active dans l'Alborz Central et la region de Teheran: Approche morphotectonique et paleoseismologique. (Ph.D. thesis). Montpellier II, Montpellier, 304p.

Nemati, M., Hatzfeld, D., Gheitanchi, M. R., Sadidkhouy, A., Mirzaei, N., 2011. Microseismicity and seismotectonics of the Firuzkuh and Astaneh faults (east Alborz, Iran). Tectonophysics 506: 11-21.

Nemati, M., Hollingsworth, J., Zhan, Z., Bolourchi, M.J., Talebian, M., 2013. Microseismicity and seismotectonics of the South Caspian Lowlands, NE Iran. Geophysical Journal International 193: 1053-1070.

Paknia, M., Ballato, P., Heidarzadeh, G., Cifelli, F., Hassanzadeh, J., Vezzoli, G., Mirzaie Ataabadi, M., Ghassemi, M. R., Mattei, M., 2021. Neogene tectono-stratigraphic evolution of the intermontane Tarom Basin: Insights into basin filling and plateau building processes along the northern margin of the Iranian Plateau (Arabia-Eurasia collision zone). Tectonics 40, e2020TC006254.

Poblet, J., Lisle, R. J., 2011. Kinematic Evolution and Structural Styles of Fold-and-Thrust Belts, In: Poblet, J., Lisle, R. J., (Eds), Kinematic Evolution and Structural Styles of Foldand- Thrust Belts. Geological Society of London, Special Publications 349: pp. 1-24.

Ramsay, J. G., and Huber, M. I., 1983. The techniques of modern structural geology. Vol. 1: Strain analysis. New York. Academic Press. 302p.

Reuter, M., Piller, W. E., Harzhauser, M., Mandic, O., Berning, B., Rogl, F., Kroh, A., Aubry, M.-P., Wielandt- Schuster, U., Hamedani, A., 2007. The Oligo- Miocene Qom Formation (Iran): Evidence for an early Burdigalian restriction of the Tethyan Seaway and closure of its Iranian gateways. International Journal of Earth Sciences 98: 627-650.

Rezaeian, M., Carter, A., Hovius, N., Allen, M. B., 2012. Cenozoic exhumation history of the Alborz Mountains, Iran: New constraints from low temperature chronometry. Tectonics 31: TC2004.

Rezaeian, M., Kuijper, C. B., van der Boon, A., Pastor-Gálan, D., Cotton, L.J., Langereis, C. G., Krijgsman, W., 2020. Post-Eocene coupled oroclines in the Talesh (NW Iran): Paleomagnetic constraints, Tectonophysics 786.

Rieben, H., 1955. The geology of the Tehran plain. American Journal of Science 253: 617-639.

Ritz, J.-F., Nazari, H., Ghassemi, A., Salamati, R., Shafei, A., Solaymani, S., Vernant, P., 2006. Active transtension inside central Alborz: a new insight into northern Iran-southern Caspian geodynamics. Geology 34: 477-480.

Ritz, J.F., 2009. Extrusion tectonics and subduction in the eastern South Caspian region since 10 Ma: Comment, Geology 37: E191-E191.

Saberi, E., Yassaghi, A., Djamour, Y., 2017. Application of geodetic leveling data on recent fault activity in Central Alborz, Iran. Geophysical Journal International 211: 751-765.

Salamati, R., 2013. Geological map of Eskadar Quadrangle Scale 1:25,000. Geological Survey of Iran

SengÖr, A. M. C., 1979. Mid-Mesozoic closure of Permo-Triassic Tethys and its implications. Nature 279: 590-593.

Shafiei Bafti, B., Dunkl, I., Madanipour, S., 2021. Timing of fluorite mineralization and exhumation events in the east Central Alborz Mountains, northern Iran: constraints from fluorite (U–Th)/He thermochronometry. Geological Magazine.

Shahidi, A. R., 2008. Evolution Tectonique du Nord de l'Iran (Alborz et Kopet-Dagh) depuis le Mésozoïque. (Ph.D. thesis). Sciences de la Terre, l'universite Pierre et Marie Curie, 500p.

Solaymani Azad, Sh., Ritz, J.-F., Abbassi M. R., 2011. Left-lateral active deformation along the Mosha-North Tehran fault system (Iran): Morphotectonics and paleoseismological investigations. Tectonophysics 497: 1-14.

SoltaniMoghadam, S., Tatar, M., Komeazi, A., 2019. An improved 1-D crustal velocity model for the Central Alborz (Iran) using Particle Swarm Optimization algorithm. Physics of the Earth and Planetary Interiors 292: 87-99..

Stampfli, G., Marcoux, J., Baud, A., 1991. Tethyan margins in space and time. Palaeogeography, Palaeoclimatology and Palaeoecology 87: 373-409.

Stampfli, G. M., Borel, G. D., 2002. A plate tectonic model for the Paleozoic and Mesozoic constrained by dynamic plate boundaries and restored synthetic oceanic isochrones. Earth and Planetary Science Letters 196: 17-33.

Stöcklin, J., Ruttner, A., Nabavi, M., 1964. New data on the Lower Paleozoic and pre-Cambrian of North Iran. Geological Survey of Iran, Report no. 1, 29p.

Stöcklin, J., 1968. Structural history and tectonics of Iran: A review. The American Association of Petroleum Geologists Bulletin 52: 1229-1258.

Stöcklin, J., 1974. Northern Iran: Alborz Mountains, In: Spencer, A., (Ed.), Mesozoic–Cenozoic orogenic belts: data for orogenic studies. Geological Society Special Publication 4: 213-234.

Talebian, M., Copley, A.C., Fattahi, M., Ghorashi, M., Jackson, J.A., Nazari, H., Sloan, R.A., Walker, R.T., 2016. Active faulting within a megacity: the geometry and slip rate of the Pardisan thrust in central Tehran, Iran. Geophysical Journal International 207: 1688-1699.

Tadayon, M., Rossetti, F., Zattin, M., Calzolari, G., Nozaem, R., Salvini, F., Faccenna, C., Khodabakhshi, P., 2018. The long-term evolution of the Doruneh Fault region (Central Iran): A key to understanding the spatio-temporal tectonic evolution in the hinterland of the Zagros convergence zone. Geological Journal 54: 1454-1479.

Tchalenko, J.S., Berberian, M., Iranmanesh, H., Bailly, M., Arsovsky, M., 1974. Tectonic framework of the Tehran region. Geological Survey of Iran. Report no 29.

Vahdati Daneshmand, F., 1991. Geological map of Amol Quadrangle Scale 1:250,000. Geological Survey of Iran.

Vahdati Daneshmand, F., Saidi, A., 1990. Geological map of Sari Quadrangle Scale 1:250,000. Geological Survey of Iran.

Verdel, C. S., 2008. Cenozoic Geology of Iran: An Integrated Study of Extensional Tectonics and Related Volcanism. (Ph.D. thesis). Pasadena, California Institute of Technology, 182p.

Verdel, C. S., Wernicke, B. P., Hassanzadeh, J., Guest, B., 2011. A Paleogene extensional arc flare-up in Iran. Tectonics 30.

Vernant, P., Nilforoushan, F., Hatzfeld, D., Abbassi, M. R., Vigny, C., Masson, F., Nankali, H., Martinod, J., Ashtiani, A., Bayer, R., Tavakoli F. and Chéry, J., 2004a. Present-day crustal deformation and plate kinematics in Middle East constrained by GPS measurements in Iran and northern Oman. Geophysical Journal International 157: 381-398.

Vernant, P., Nilforoushan, F., Chéry, J., Bayer, R., Djamour, Y., Masson, F., Nankali, H., Ritz, J.-F., Sedighi, M., Tavakoli, F., 2004b. Deciphering oblique shortening of central Alborz in Iran using geodetic data. Earth and Planetary Science Letters 223: 177-185.

Wheeler, J. O., Aitken, J. D., Berry, M. J., Gabrielse, H., Hutchinson, W. W., Jacoby, W. R., Monger, J.W.H., Niblett, E. R., Norris, D. K., Price, R. A., Stacey, R. A., 1972. The Cordilleran structural province. In: Price, R. A., Douglas, R. J. W., (Eds), Variations in Tectonic Styles in Canada. Geological Association of Canada, Special Paper, 11: 1-82.

Wilmsen, M., Fürsich, F. T., Seyed-Emami, K., Majidifard, M. R., Taheri, J., 2009. The Cimmerian orogeny, in northern Iran: Tectono-stratigraphic evidence from the foreland. Terra Nova 21: 211-218.

Yassaghi, A., 2005. The effect of deep-seated Transversal faults on structural evolution of west-central Alborz mountains. Geophysical Research Abstracts, v. 7, 00504, SRef-ID: 1607-7962/gra/ EGU05-A-00504. © European Geosciences Union

Yassaghi, A., Madanipour, S., 2008. Influence of a transverse basement fault on along-strike variations in the geometry of an inverted normal fault: Case study of the Mosha fault, central Alborz Range, Iran. Journal of Structural Geology 30: 1507-1519.

Yassaghi, A., Naeimi, A., 2011. Structural analysis of the Gachsar subzone in central Alborz range; constrain for inversion tectonics followed by the range transverse faulting, International Journal of Earth Sciences 100: 1237-1249.

Yousefi, E., Friedberg, J. L., 1977. Aeromagnetic map of Semnan (1:250000). Geological survey of Iran, Tehran, Iran.

Yuan, N., Huiwen, X., Hongwei, Y., Yong, L., Wei, W., 2018. Effect of basement structure and salt tectonics on deformation styles along strike: An example from the Kuqa fold–thrust belt, West China. Tectonophysics 730: 114-131.

Yin, A., 2006. Cenozoic tectonic evolution of the Himalayan orogen as constrained by along-strike variation of structural geometry, exhumation history, and foreland sedimentation. Earth-Science Reviews 76: 1-131.

Zanchi, A., Berra, F., Mattei, M., Ghassemi, M. R., Sabouri, J., 2006. Inversion tectonics in central Alborz, Iran. Journal of Structural Geology 28: 2023-2037.

Zanchi, A., Zanchetta, S., Berra, F., Mattei, M., Garzanti, E., Molyneux, S., Nawab, A., Sabouri, J., 2009. The Eo-Cimmerian (Late? Triassic) orogeny in North Iran, In: Brunet, M.-F., Wilmsen, M., Granath, J. W. (Eds.), South Caspian to Central Iran Basins. The Geological Society, London, Special Publications 312: 31-55.